Supplementary Information for

Inhibiting APOBEC3 Activity with Single-Stranded DNA Containing 2'-Deoxyzebularine analogues

Maksim V. Kvach[†,#], Fareeda M. Barzak[†,#], Stefan Harjes[†,#], Henry A. M. Schares[§,#], Geoffrey B. Jameson[†,‡], Alex M. Ayoub[§,], Ramkumar Moorthy[§,], Hideki Aihara[‖], Reuben S. Harris[‖,⊥], Vyacheslav V. Filichev[†,‡*], Daniel A. Harki[§,*], Elena Harjes[†,‡*]

[†]Institute of Fundamental Sciences, Massey University, Private Bag 11 222, Palmerston North, New Zealand
[‡]Maurice Wilkins Centre for Molecular Biodiscovery, 1142, Auckland, New Zealand
[§]Department of Medicinal Chemistry and [‖]Department of Biochemistry, Molecular Biology, and Biophysics, University of Minnesota, Minneapolis, MN 55455, United States
[⊥] Howard Hughes Medical Institute, University of Minnesota, Minneapolis, MN 55455, USA.

[#] These authors contribute equally to this work.

*E-mail: e.harjes@massey.ac.nz, daharki@umn.edu, v.filichev@massey.ac.nz

Table of Contents

1. Synthesis of 2'-deoxyzebularine (dZ), its phosphoramidite and oligonucleotides containing dZ and dZ^{Me}.

1.1. s

Reagents from commercial suppliers were used without further purification. Pyridine, Et_3N and CH_2Cl_2 were freshly distilled from CaH_2. Hoffer's chlorosugar **1** was prepared as described.[1] ^1H (400.1 or 500.1 MHz), ^{13}C (100.6 or 125.8 MHz) and ^{31}P (202.5 MHz) NMR spectra were obtained with Bruker Avance 400 or Avance 500 MHz spectrometers and referenced to residual solvent signals ($CDCl_3$: 7.26 ppm for ^1H and 77.16 ppm for ^{13}C, d_6-DMSO: 2.50 ppm for ^1H and 39.52 ppm for ^{13}C according to reference[2] or 85% aq. H_3PO_4 external standard (0.0 ppm for ^{31}P). ^1H NMR coupling constants are reported in Hertz (Hz) and refer to apparent multiplicities. The assignments of signals were done using 2D homonuclear ^1H-^1H COSY, NOESY and heteronuclear ^1H–^{13}C HMQC or HSQC, and HMBC spectra. NMR spectra were processed in Spinworks version 4.1 (developed by Dr. Kirk Marat, Department of Chemistry, University of Manitoba). High-resolution electrospray mass spectra were recorded on a Thermo Scientific Q Exactive Focus Hybrid Quadrupole-Orbitrap mass spectrometer. Ions generated by ESI were detected in negative ion mode. Total ion count (TIC) was recorded in centroid mode over the *m*/*z* range of 500-3,000 and analyzed using ThermoXcalibur Qual Browser. Analytical thin-layer chromatography was performed on Kieselgel 60 F_{254} precoated aluminum plates (Merck). Silica gel column chromatography was performed using silica gel 60 (40–63 µm). Oligonucleotide syntheses were carried out on a MerMade-4 DNA/RNA synthesizer (BioAutomation) or on an Applied Biosystems 394 DNA/RNA synthesizer on a 1-5 µmol scale using standard manufacturer's protocol. 'Saltless buffer' used for oligonucleotide desalting consists of 10 µM Tris-HCl (pH 8.0), 1 µM EDTA and 0.001% w/v NaN_3.

1.2. Synthetic procedures

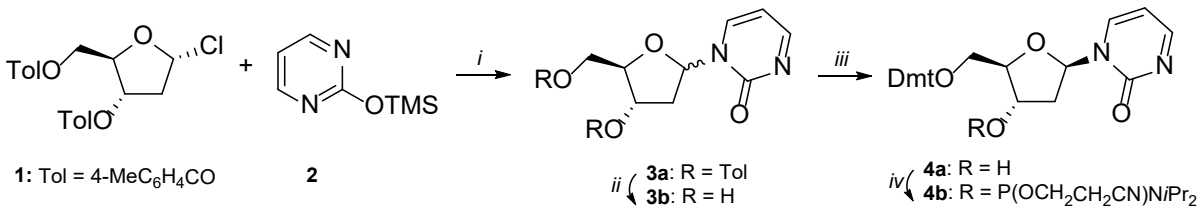

Scheme S1. Reagents and conditions: *i*, $CHCl_3$, distill., 10 min, 54%, α/β=12:88 (**3a**); *ii*, 28% aq. ammonia, MeOH, 48 h, (**3b**); *iii*, 4,4'-dimethoxytritylchloride, pyridine, 0°C→r.t., overnight, 54% (**4a**); *iv*, *N*,*N*-di*iso*propylamino-2-cyanoethoxychlorophosphine, Et_3N, CH_2Cl_2, 30 min, 88% (**4b**).

2-Trimethylsilyloxypyrimidine (**2**) was prepared as previously described.[3] Suspension of 2-hydroxypyrimidine hydrochloride (13.25 g, 100.0 mmol) and catalytic amounts of $(NH_4)_2SO_4$ in hexamethyldisilazane (37.2 mL, 179.0 mmol) was refluxed for 4h. Reaction mixture was fractionally distilled under reduced pressure to yield 2-trimethylsilyloxypyrimidine (15.33 g, 91%) as cloudy liquid. B.p. (10 mbar) 82-83°C. ^{1}H NMR (500.1 MHz, $CDCl_3$) δ 8.46 (d, 2H, J = 4.8 Hz, H-4,6), 6.89 (t, 1H, J = 4.8 Hz, H-5), 0.38 (s, 9H, H-CH_3). ^{13}C NMR (125.7 MHz, $CDCl_3$) δ 163.7 (C2), 159.3 (2C, C4), 114.9 (C5), 0.1 (3C, CH$_3$).

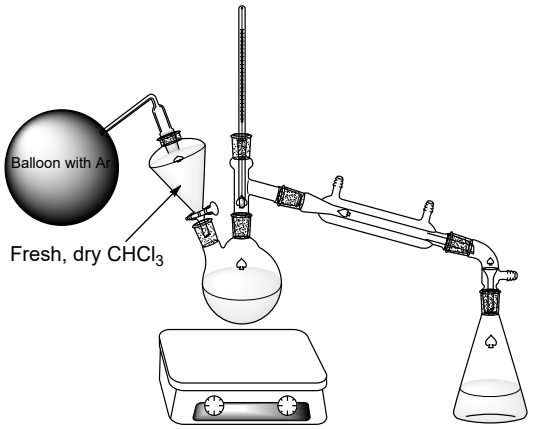

Chart S1. Set-up used for the synthesis of **3a**.

3',5'-Di-*O*-(p-toluoyl)-2'-deoxyzebularine (3a) was prepared by silyl-Hilbert-Johnson reaction with modification described earlier.[4] In a round bottom two-neck flask (**Chart S1**) was placed dry $CHCl_3$ (6 mL) and distillation started with a speed 2-2.5 mL/min. Fresh chloroform was added through dropping funnel with the same speed to keep the reaction volume (6 mL) constant. 2-Trimethylsilyloxypyrimidine **2** (1.51 g, 9.0 mmol) followed by Hoffer's chlorosugar **1** (1.17 g, 3.0 mmol) were added and distillation was continued for 10 min. keeping reaction volume constant. Solvent was rotary evaporated and residue was flash chromatographed on silica eluting with a step gradient of acetone (0→30%) in CH_2Cl_2 to yield **3a** (0.72 g, 54%) with α/β ratio 12:88 as a colorless foam. This mixture of anomers was used in the next step without isolation of pure β-anomer. R_f 0.58 (α-anomer), 0.51 (β-anomer) (1-BuOH).

5'-*O*-(4,4'-Dimethoxytrityl)-2'-deoxyzebularine (4a) was prepared similarly to the procedure described earlier.[5] 3',5'-Toluoyl protected 2'-deoxynucleoside **3a** with α/β ratio 12:88 (6.10 g, 13.6 mmol) was dissolved in MeOH (500 mL) and aq. ammonia (28%, 50 mL) was added in one portion. Reaction mixture was stirred at room temperature for 48 h, rotary evaporated, co-evaporated with H_2O (2 × 200 mL), abs. EtOH (200 mL)

and abs. pyridine (200 mL) to afford deprotected nucleoside **3b** as a yellowish oil. It was dissolved in abs. pyridine (140 mL), cooled to 0°C and 4,4'-dimethoxytritylchloride (5.06 g, 14.9 mmol) was added. Reaction was stirred overnight on a melting ice bath, evaporated *in vacuo*, residue was dissolved in CH_2Cl_2 (250 mL), washed with H_2O (250 mL), satd. $NaHCO_3$ (250 mL) and brine (250 mL), filtered through Na_2SO_4 and rotary evaporated *in vacuo*. Flash chromatography on silica eluting with a step gradient of 2-propanol (0→7%) in a mixture of CH_2Cl_2/Et_3N 99:1 (v/v) afforded pure β-anomer **4a** (3.80 g, 54% on **3a**) as a yellowish foam after rotary evaporation of solvent. DMT-protected α-anomer eluted after the β-anomer and was not collected.

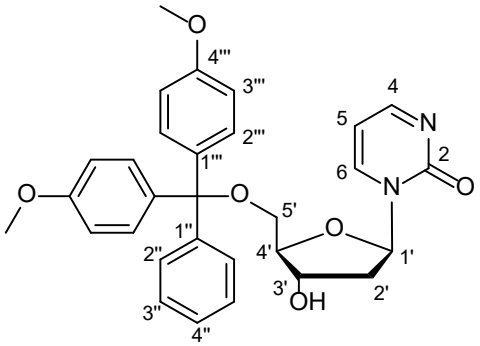

R_f 0.21 (α-anomer), 0.26 (β-anomer) (Et_3N/2-propanol/CH_2Cl_2 1:5:94 v/v/v). ^{1}H NMR (500.1 MHz, d_6-DMSO) δ 8.54 (dd, 1H, $J_{4,5}$ = 4.1 Hz, $^4J_{4,6}$ = 2.8 Hz, H-4), 8.23 (dd, 1H, $J_{5,6}$ = 6.7 Hz, $^4J_{4,6}$ = 2.8 Hz, H-6), 7.40-7.35 (m, 2H, H-2''), 7.34-7.28 (m, 2H, H-3''), 7.27-7.21 (m, 1H, H-4''), 7.26, 7.25 (2d, 4H, $J_{2''',3'''}$ = 9.0 Hz, H-2'''), 6.90 (d, 4H, $J_{2''',3'''}$ = 9.0 Hz, H-3'''), 6.25 (dd, 1H, $J_{5,6}$ = 6.7 Hz, $J_{4,5}$ = 4.1 Hz, H-5), 6.07 (app. t, 1H, J = 5.9 Hz, H-1'), 5.42 (d, 1H, $J_{3',OH}$ = 4.7 Hz, H-O*H*), 4.31 (app. quint, 1H, J = 5.3 Hz, H-3'), 4.02 (q, 1H, J = 4.1 Hz, H-4'), 3.74 (s, 6H, H-CH_3), 3.33-3.25 (m, 2H, H-5'), 2.47-2.40 (m, 1H, H-2'α), 2.13 (app. dt, 1H, $J_{2'\alpha,2'\beta}$ = 13.4 Hz, J = 5.9 Hz, H-2'β). ^{13}C NMR (125.8 MHz, d_6-DMSO) δ 166.0 (C4), 158.2 (2C, C4'''), 154.6 (C2), 144.6 (C1''), 143.7 (C6), 135.4 and 135.2 (2C, C1'''), 129.8 and 129.7 (4C, C2'''), 127.9 (2C, C3''), 127.7 (2C, C2''), 126.8 (C4''), 113.28 and 113.27 (4C, C3'''), 103.7 (C5), 86.8 (C1'), 86.0 (C4'), 85.9 (*C*Ar$_3$), 69.4 (C3'), 62.8 (C5'), 55.1 (2C, *C*H$_3$), 40.9 (C2').

5'-*O*-(4,4'-Dimethoxytrityl)-2'-deoxyzebularine-3'-*O*-(2-cyanoethyl-*N*,*N*-di*iso*propylphosphoramidite) (4b) was prepared similarly to the protocol described earlier.[5] 5'-*O*-DMT-2'-deoxyzebularine **4a** (2.70 g, 5.25 mmol) was co-evaporated with abs. CH_2Cl_2 (100 mL), dissolved in abs. CH_2Cl_2 (50 mL) and Et_3N (1.10 mL, 7.9 mmol) followed by addition of *N*,*N*-di*iso*propylamino-2-cyanoethoxychlorophosphine (1.61 g, 6.8 mmol) under argon. After 30 min stirring reaction was complete (TLC in CH_2Cl_2/AcOEt/Et_3N 45:45:10), reaction mixture was diluted with CH_2Cl_2 (100 mL), washed with H_2O (100 mL), satd. $NaHCO_3$ (3 × 100 mL), filtered through Na_2SO_4 and rotary evaporated. The residue was purified by flash chromatography on silica (50 mL, packed in CH_2Cl_2/AcOEt/Et_3N 45:45:10 and washed with 400 mL CH_2Cl_2/AcOEt 95:5)

eluting with a step gradient of AcOEt (5→30%) in CH_2Cl_2. Fractions with the product were collected, rotary evaporated *in vacuo*, co-evaporated with abs. CH_2Cl_2 and dried *in vacuo* to yield **4b** (3.30 g, 88%) as a slightly yellowish foam.

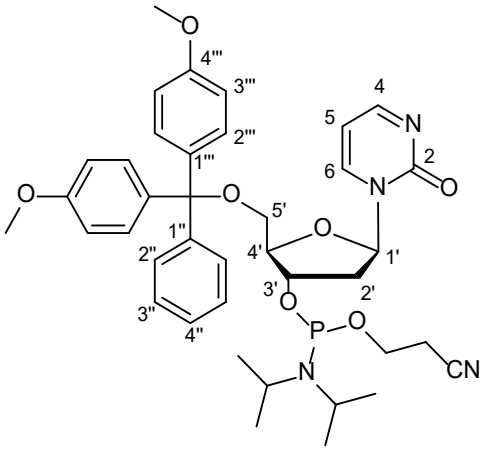

R_f 0.72, 0.66 (diastereomers, AcOEt/CH_2Cl_2 3:7 v/v, TLC pretreated with Et_3N/Hex 1:9 v/v and dried). ^{1}H NMR (500.1 MHz, d_6-DMSO) δ 8.552, 8.549 (2dd, 1H, $J_{4,5}$ = 4.1 Hz, $^4J_{4,6}$ = 2.8 Hz, H-4); 8.27, 8.25 (2dd, 1H, $J_{5,6}$ = 6.7 Hz, $^4J_{4,6}$ = 2.8 Hz, H-6); 7.40-7.34 (m, 2H, H-2''); 7.34-7.28 (m, 2H, H-3''); 7.28-7.20 (m, 5H, H-2''',4''); 6.93-6.85 (m, 4H, H-3'''); 6.27 (dd, 1H, $J_{5,6}$ = 6.7 Hz, $J_{4,5}$ = 4.1 Hz, H-5); 6.10 (dd, J = 6.5 Hz, J = 5.4 Hz), 6.07 (app. t, J = 5.9 Hz) (1H, H-1'); 4.58-4.48 (m, 1H, H-3'); 4.17 (q, J = 4.0 Hz), 4.12 (q, J = 4.2 Hz) (1H, H-4'); 3.79-3.60 (m, 2H, CH_2CH$_2$CN); 3.74 (s), 3.73 (br. s) (6H, OCH$_3$); 3.60-3.40 (m, 2H, NCHCH$_3$); 3.36-3.30 (m, 2H, H-5'); 2.75, 2.65 (2t, 2H, J = 5.9 Hz, CH$_2$CH_2CN); 2.63-2.51 (m, 1H, H-2'α); 2.34-2.25 (m, 1H, H-2'β); 1.13, 1.11, 1.10 (3d, J = 6.8 Hz), 1.00 (d, J = 6.7 Hz) (12H, NCHCH_3). ^{13}C NMR (125.8 MHz, d_6-DMSO) δ 166.22, 166.18 (C4); 158.2 (2C, C4'''); 154.55, 154.54 (C2); 144.53, 144.51 (C1''); 143.9, 143.7 (C6); 135.22, 135.21, 135.08, 135.04 (2C, C1'''); 129.8, 129.7 (4C, C2'''); 127.93, 127.70, 127.67 (4C, C2'',3''); 126.87, 126.85 (C4''); 118.9, 118.8 (CN); 113.2 (4C, C3'''); 103.80, 103.77 (C5); 86.87, 86.86 (C1'); 86.11, 86.05 (*C*Ar$_3$); 85.1 (d, $^3J_{C,P}$ = 4.0 Hz), 84.8 (d, $^3J_{C,P}$ = 5.8 Hz) (C4'); 72.1 (d, $^2J_{C,P}$ = 17.5 Hz), 71.5 (d, $^2J_{C,P}$ = 16.1 Hz) (C3'); 62.4, 62.2 (C5'); 58.4 (d, $^2J_{C,P}$ = 18.7 Hz), 58.3 (d, $^2J_{C,P}$ = 18.4 Hz) (*C*H$_2$CH$_2$CN); 55.08, 55.07 (2C, O*C*H$_3$); 42.7 (d, 2C, $^2J_{C,P}$ = 12.3 Hz, N*C*HCH$_3$); 39.8, 39.6 (C2'); 24.39, 24.33, 24.31, 24.30, 24.25, 24.20 (4C, NCH*C*H$_3$); 19.9 (d, $^3J_{C,P}$ = 6.9 Hz), 19.8 (d, $^3J_{C,P}$ = 7.2 Hz) (CH$_2$*C*H$_2$CN). ^{31}P NMR (202.5 MHz, d_6-DMSO, ref. 85% H_3PO_4) δ 149.0, 148.8 in ~1:1 ratio.

1.3. Synthesis of dZ and dZ^{Me} modified oligos

1.3.1. Synthesis of oligos 7-9

Oligonucleotides were prepared on a MerMade-4 DNA/RNA synthesizer (BioAutomation) on a 5 µmol scale using standard manufacturer's protocol. Phosphoramidite **4b** and commercially available phosphoramidite of 5-methyl-2'-deoxyzebularine were used in the synthesis of modified oligonucleotide sequences (**Table S1**). Coupling time of 2'-deoxyzebularines was increased to 5 min. The final detritylation step was omitted and DMT-ON oligonucleotides were cleaved from the solid support and deprotected with conc. ammonia solution (1.0 mL) at room temperature for 24 h. After filtering, an aq. solution of 0.3 M $LiClO_4$ (0.5 mL) was added and oligonucleotides were precipitated with acetone (14 mL). The DMT-ON oligonucleotides were isolated by reversed-phase HPLC on 250/10 mm, 5 µm, 300 Å C18 column (Phenomenex) in a gradient of CH_3CN (0→60% for 15 min, 4.6 mL/min) in 0.1 M TEAA buffer (pH 7.0) with a detection at 260 nm. DMT-ON oligonucleotides were freeze-dried and manually detritylated with 80% aq. AcOH (2 mL) during 20 min at room temperature. 3 M AcONa solution (0.5 mL) was then added and oligonucleotides were precipitated with 2-propanol (11 mL). DMT-OFF oligonucleotides were purified by RP-HPLC on 250/4.6 mm, 5 µm, 300 Å C18 column (Phenomenex) in a gradient of CH_3CN (0→25% for 20 min, 1.3 mL/min) in 0.1 M TEAA buffer (pH 7.0). Fractions containing desired oligonucleotides were combined, freeze-dried, dissolved in milli-Q water (1.5 mL) and desalted on a NAP-25 column (GE Healthcare) against 'saltless buffer'. Pure products were quantified by measuring absorbance at 260 nm, analyzed by ESI-MS (Table 1-SI) and concentrated by freeze-drying.

1.3.2. Synthesis of oligo-15

DMT-protected phosphoramidite of dZ synthesized according to the previously published procedure[5, 6] was incorporated into 5'-TTTT**dZ**AT using an Applied Biosystems 394 DNA/RNA synthesizer on 1 µmole scale using a published protocol.[7] The 2'-deoxyzebularine phosphoramidite was incorporated into the oligonucleotide by a manual coupling following deprotection (trityl-off) of the 3'-nucleotide using the technique reported previously by our group.[7] The oligonucleotide was purified by HPLC (Agilent 1200 series instrument equipped with a diode array detector) using PLRP-S column (5 µm, 100 Å, 4.6 × 150 mm, Agilent Technologies). The analysis method (1 mL/min flow rate) involved isocratic 98% Solvent A (100 mM TEAA; pH 7.0) and 2% Solvent B (1:1 of 100 mM TEAA/MeCN) (0−5 min) followed by two linear gradient to 15% Solvent B (5−15 min) and 35% Solvent B (15−50 min) and finally a linear gradient to 80% Solvent B (50−60 min). After purification, the oligonucleotide was desalted with DNase/RNase-free H_2O using Illustra NAP-5 columns (Sephadex G-25 DNA grade). The

desalted oligonucleotide was characterized by LC-MS (Table 1-SI) using our previously reported method.[7]

Table S1. TSA-modified Oligos synthesised and purified using protocols described above in 1.2 and 1.3.

Name	**Sequence 5'→3'**	**ESI-MS $[M-H]^-$ found/calcd**
Oligo-7	ATTCC**dZ**AATT	2944.5 / 2944.5
Oligo-8	ATTCC**dZ^{Me}**AATT	2958.5 / 2958.5
Oligo-9	ATTT**dZ**ATTT	2661.5 / 2661.5
Oligo-15	TTTT**dZ**AT	2046.2 / 2046.3

2. Protein expression and purification for ITC and NMR kinetic assays

2.1. A3 enzymes and substrate preferences

In this study we focus on human A3A and the catalytically active C-terminal domains of A3B ($A3B_{CTD}$) and A3G ($A3G_{CTD}$) (sequences in **Fig. S3**). Wild type hA3A and $hA3B_{CTD}$ expressed in human cells were used in fluorescence-based activity assay. Because wild type $A3B_{CTD}$ ($wtA3B_{CTD}$) does not express well, when purified from *E. coli*, we used derivatives of $A3B_{CTD}$ ($A3B_{CTD}$-DM, $A3B_{CTD}$-QM-ΔL3, and $A3B_{CTD}$-QM-ΔL3-AL1swap).[8] $A3B_{CTD}$-QM-ΔL3-AL1swap is the most active of all $A3B_{CTD}$ listed mutants; $A3B_{CTD}$-DM is less active but the sequentially closest to $wtA3B_{CTD}$. $A3B_{CTD}$-QM-ΔL3-AL1swap, $A3B_{CTD}$-DM, and $A3G_{CTD}$ were used in NMR-based activity and inhibition assays to test dZ-containing oligos. $A3B_{CTD}$-QM-ΔL3 has very low activity in our NMR assay, and therefore was used in thermal shift assay together with its inactivated mutant $A3B_{CTD}$-QM-ΔL3-E255A.[9] Additionally, inactivated A3A-E72A, was used to study A3A binding to ssDNA.

2.2. Human A3A-E72A expressed in *E. coli*

For ITC experiments, human APOBEC3A (1-199, Uniprot code P31941) was cloned as the inactive E72A mutant with a His_6 C-terminal fusion tag into an expression vector (pETite, Lucigen) and expressed in *Escherichia coli* BL21 DE3 cells (Hi-Control, Lucigen). The expression medium was supplemented with 100 µM Zn^{2+}. Cells were grown in 5 L shake flasks at 37 °C and shortly before induction cooled to 20 °C. Protein expression was induced with 0.25 mM IPTG and protein was expressed at 20 °C overnight. Cells were harvested and resuspended in the following buffer: 25 mM sodium phosphate, pH 7, 500 mM sodium chloride, 5 mM β-mercaptoethanol and 0.2 mM Na_2-EDTA or optimized buffer (25 mM sodium phosphate, 500 mM sodium chloride, 5 mM β-mercaptoethanol and 0.2 mM Na_2-EDTA at pH 6.0 plus 300 mM choline acetate and 0.1 mM LysoFos Choline 12 (Anatrace) as described earlier).[10] Cells were disrupted by sonication or French press, with about twice the yields for the latter method. Lysate was cleared by centrifugation (25 min, 4 °C, 38 000 *g*) and the supernatant was collected. The protein was purified by metal affinity chromatography. After loading the supernatant, a Ni^{2+}-NTA affinity column (BioRad) was washed three times with 10 column volumes of one of the above buffers containing 50 mM imidazole followed by one wash with 200 mM imidazole and eluted with 1 M imidazole. The eluted protein was loaded onto a gel filtration column (Highload 16⁄600 Superdex 75 pg) and the peak shortly before 100 mL elution volume was collected. The protein was concentrated to about 100 µM using Centricons (Vivaspin 20, 10 kDa MWCO) and aliquots were frozen at -70 °C in the optimized buffer.

Fluorescence polarization assays were performed with recombinant (purified from *E. coli* strain BL21[DE3]), A3A (amino acids 1-195, expressed using the pGEX vector as a GST-fusion)[9] with the catalytic glutamic acid mutated to alanine (E72A) to render the enzyme unable to deaminate substrate. Before use in the fluorescence polarization assay, protein buffer was exchanged from protein storage buffer to FP assay buffer.

2.3. Human $A3B_{CTD}$-QM-ΔL3 and $A3B_{CTD}$-DM mutants expressed in *E. coli*

A3B C-terminal domain (residues 187 to 378, UniProt ID Q9UH17) was cloned into pET24a vector (Novagen) to produce $A3B_{CTD}$ proteins with a non-cleavable C-terminal His_6-tag (LEHHHHHH).[9] Several derivative constructs previously reported[8] were used in this study, $A3B_{CTD}$ -QM-ΔL3, $A3B_{CTD}$ -QM-ΔL3-E255A were expressed in *E. coli* strain BL21(DE3) (Lucigen), and $A3B_{CTD}$ -QM-ΔL3-AL1swap expressed in the *E. coli* strain C41(DE3)pLysS (Lucigen). *E. coli* culture was grown at 37 °C in LB medium, once mid-log growth phase was established the culture supplemented with 100 µM zinc chloride, before inducing protein expression by the addition of isopropyl β-D-1-thiogalactopyranoside (IPTG) at a final concentration of 0.5 µM and incubating overnight at 18 °C.

The cell culture was harvested via centrifugation and resuspended in 50 mM Tris-HCl (pH 7.4), 0.5 M NaCl, and 5 mM β-mercaptoethanol 50, lysed by sonication and soluble protein was purified through a Ni^{2+}-NTA affinity column (BioRad) eluting the protein with 500 mM imidazole. The eluted proteins were loaded through a Superdex 75 10/300 GL column (GE Healthcare) using ÄKTA protein purification system (GE Healthcare) producing a monomeric peak between 90 and 120 mL (see for example **Chart S2**). The purified proteins were concentrated using Centricons (Vivaspin 20, 10 kDa MWCO) and aliquots were frozen at -80 °C.

$A3B_{CTD}$ -DM was expressed and purified as reported in the recent paper.[8]

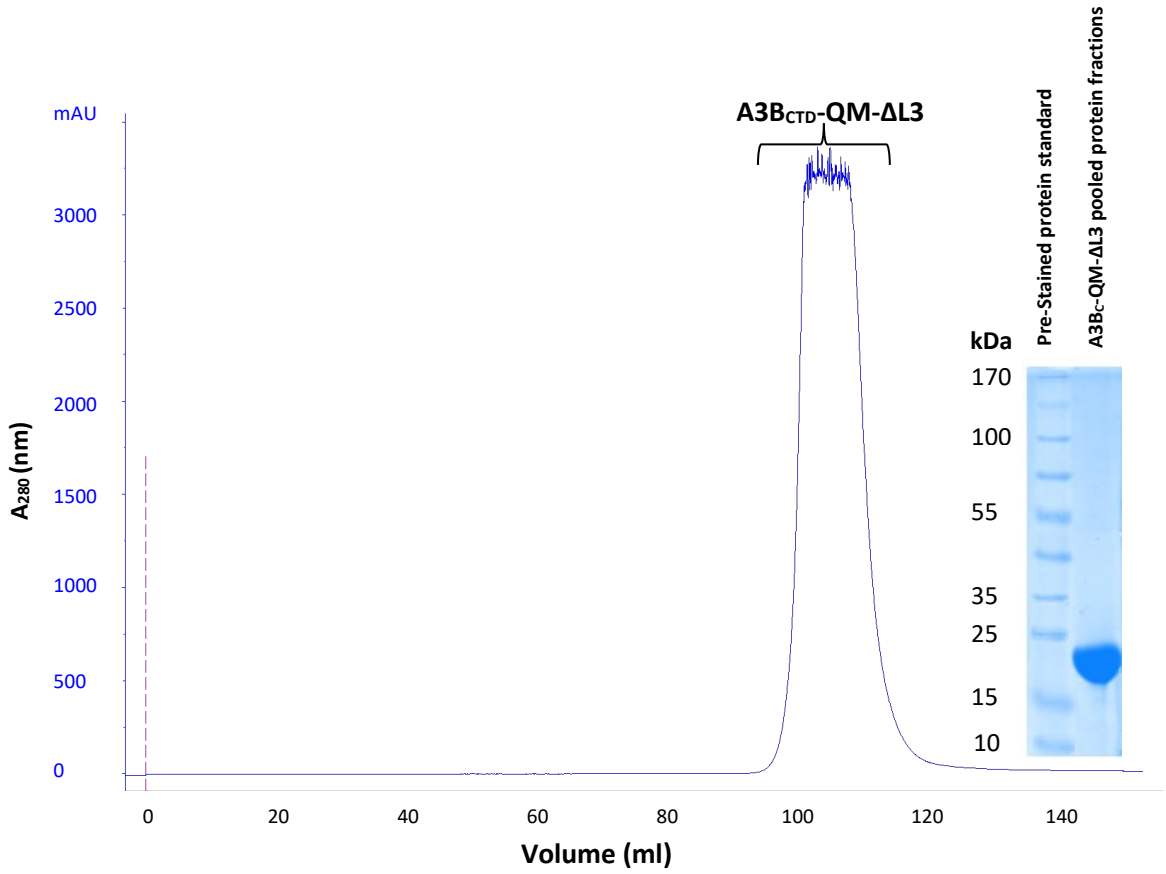

Chart S2. Profile of size-exclusion chromatography and SDS-PAGE of A3B$_{CTD}$-QM-ΔL3.

2.4.Human A3G$_{CTD}$ expressed in *E. coli*

A3G$_C$ (191-384, NM_021822, wt) was purified as described.[11] The glutathione S-transferase (GST)-fused A3G$_{CTD}$ was expressed in *Escherichia coli* BL21(DE3) cells overnight at 17°C. After harvesting, the cells were resuspended in 50 mM sodium phosphate buffer (pH 7.4) and lysed by sonication. After ultracentrifugation at 25,000 *g* for 10 min, the supernatant was added to glutathione (GSH)-Sepharose, which was subsequently washed. For kinetic analysis, the GST fusion protein was eluted from the Sepharose matrix with 100 mM GSH in phosphate buffer. By using filtration at 4,000 *g*, the buffer was changed to a solution containing 75 mM sodium phosphate and 75 mM citrate, at pH 5.5.

3. Affinity (binding) assays

3.1. Fluorescence polarization assay

The assay buffer consisted of 2-(*N*-morpholino)ethanesulfonic acid (MES; 50 mM, aq.), NaCl (100 mM, aq.), tris(2-carboxyethyl)phosphine (TCEP; 2 mM, aq.), and 3-[(3-cholamidopropyl)-dimethylammonio]-1-propanesulfonate (CHAPS; 4 mM, aq.) at pH 6.0. 15 µM stock solutions of fluorescent tracer 5'-(6-FAM)TTTTCAT (Integrated DNA Technologies; MW = 2,598.3 g/mol) in molecular biology grade water were diluted to 15 nM in assay buffer. All FP experiments were performed with a 10 µL assay volume in black round bottom low-volume 384-well plates (Corning 4514). A direct binding experiment (**Chart S3**) was first performed to determine the K_d of 5'-(6-FAM)TTTTCAT-3' to A3A-E72A by serially diluting the protein (1:1, 10 µM starting concentration) and incubating with constant concentration (15 nM) of fluorescent tracer. Plates were incubated at room temperature for 30 minutes, gently shaken for 1 minute, and then analyzed for fluorescence polarization on a BioTek Synergy 2 instrument (using standard instrument settings) with an excitation wavelength of 485 (20) nm, an emission wavelength of 528 (20) nm, and the top optics position at 510 nm. The resulting anisotropy values were fit using the one-site binding (hyperbola) function in GraphPad Prism 7.0 to obtain the K_d of the fluorescent tracer. The directly measured K_d was 18.2 ± 1.0 nM (**Chart S3**). This value was used for all further calculations.

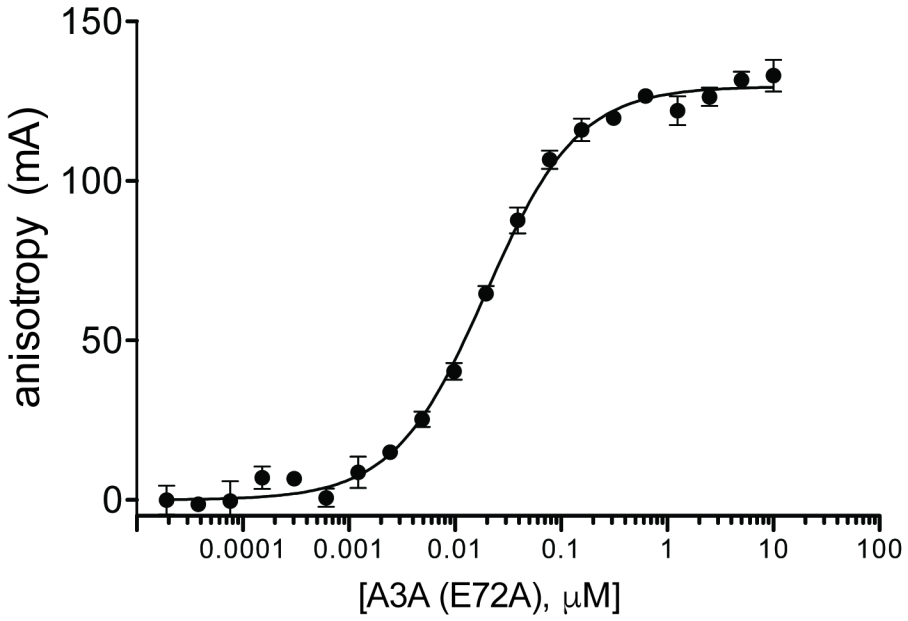

Chart S3. Fluorescence polarization direct binding assay of A3A-E72A with 5'-(6-FAM) TTT TCA T yielding a K_d of 18.2 ± 1.0 nM.

Competition binding experiments were then performed with the pre-bound fluorescent tracer and various test ligands to quantify their binding affinities. To initiate competition binding experiments, the SB_{80} (concentration of A3A-E72A at which 80% of the tracer is bound) was calculated from the K_d data.[12] Stock solutions (10 mM) of competitor oligonucleotides in molecular biology grade water were serially diluted into assay buffer from 250 µM to 200 pM with constant protein (SB_{80}) and fluorescent tracer (15 nM). The anisotropy values were then fit to GraphPad Prism log(inhibitor) vs. response – variable slope (four parameters) function after manual baseline correction to obtain IC_{50} values for each compound (**Table 1**, main text, **Fig. S2**). The IC_{50} values were then converted to K_d^{FP} values using the Kenakin equation[13, 14] (**Equation 1**) and the K_d determined from the initial direct binding experiment of the fluorescent tracer. Here, K_d^{FP} is the indirectly determined dissociation constant (**Table 1**) of the competitor oligonucleotide. Please note that although the Kenakin equation is more frequently utilized to convert IC_{50} values to K_i values, we have designated these as dissociation constants, K_d^{FP}, since the experiment is based on ligand binding and tracer dissociation, and the enzyme is catalytically inactive, which is consistent with other methods.[15] The calculated error (SEM) from the direct binding (K_d determining) experiment was propagated through to the K_d^{FP} error calculations (SEM).

(Equation 1)
$$K_{\mathrm{d}}{}^{\mathrm{FP}} = \frac{(L_b)(IC_{50})(K_d)}{\left[(L_o)(R_o) + [L_b(L_b + R_o - L_o - K_d)]\right]}$$

Where 'L_b' = bound tracer concentration, 'L_o' = total tracer concentration, 'R_o' = total protein concentration, 'L_b' = bound tracer concentration using Equations 2 and 3 to calculate these parameters:

(Equation 2)
$$\text{Bound/Free ratio of Tracer, } y_o = \frac{L_b}{\left(L_o - L_b\right)}$$

(Equation 3)
$$\text{Fraction of Tracer Bound, } F_o = \frac{L_b}{L_o}$$

We then measured the reliability of the A3A-E72A fluorescence polarization assay by measuring the Z' as recommended for assay validation.[16] Fluorescence polarization assays were performed as described above. Alternating maximum (max), medium (mid), and minimum (min) signal values were distributed by column in a standard interleaved-signal 384 well format. Max signal value wells consisted of A3A-E72A protein (SB_{80}) and fluorescent tracer (15 nM) in assay buffer. Mid signal value wells consisted of protein (SB_{80}), fluorescent tracer (15 nM), and the unlabeled competitor

(5'-TTT TCA T) at 283 nM. Min signal value wells consisted of only fluorescent tracer in assay buffer. Resulting anisotropy values were used to calculate a *Z*' value for each plate using Equation 4. *Z*' scores from all plates on all days were averaged to obtain the final *Z*' value of 0.57, which is above the recommended acceptance criterion of ≥ 0.4.[16]

(Equation 4) $$Z' = \frac{\left(AVG_{\max} - 3SD_{\max} / \sqrt{n}\right) - \left(AVG_{\max} + 3SD_{\min} / \sqrt{n}\right)}{AVG_{\max} - AVG_{\min}}$$

3.2. Isothermal titration calorimetry

Desalted unmodified DNA oligonucleotides were purchased (Integrated DNA Technologies) at 1 or 5 µmol synthesis scale and dissolved in one of the buffers described below to give 10 mM solutions.

ITC experiments (**Charts S4 - S12**) were conducted at 25 °C using a Micro-Cal ITC200 (now Malvern Instruments) isothermal titration calorimeter. A3A-E72A (130 µM in high salt or 33 µM in medium salt buffer) or $A3B_{CTD}$-QM-ΔL3-AL1swap (100 µM, activity assay buffer) was titrated in corresponding buffer. DNA oligonucleotides at 1.6 mM (for A3A-E72A) or 300 µM (for $A3B_{CTD}$-QM-ΔL3-AL1swap) concentration were added in 18 steps at 2.0 µL each (plus a first addition with reduced volume of 0.4 µL to prevent dilution of the DNA in the syringe due to the long wait before the start of the experiment). Oligos and the enzymes were dialyzed against the appropriate buffer. Buffers used are given below:

For A3A-E72A: High salt buffer consists of 25 mM sodium phosphate, 500 mM NaCl, 300 mM choline acetate, 5 mM β-mercaptoethanol and 0.2 mM Na_2-EDTA, pH 6.0 or medium salt buffer consists of 50 mM MES, 100 mM NaCl, 2.0 mM tris(2-carboxyethyl)phosphine, pH 6.0.

For $A3B_{CTD}$-QM-ΔL3-AL1swap**:** Activity assay buffer consists of 50 mM citrate-phosphate buffer, 200 mM NaCl, 2 mM β-mercaptoethanol, pH 5.5.

Analysis of ITC data was performed with Origin 7 ITC200 software, raw data were fitted to a one-site binding model producing Δ*H*, Δ*S* and K_a values (**Table S2**).

ITC data:

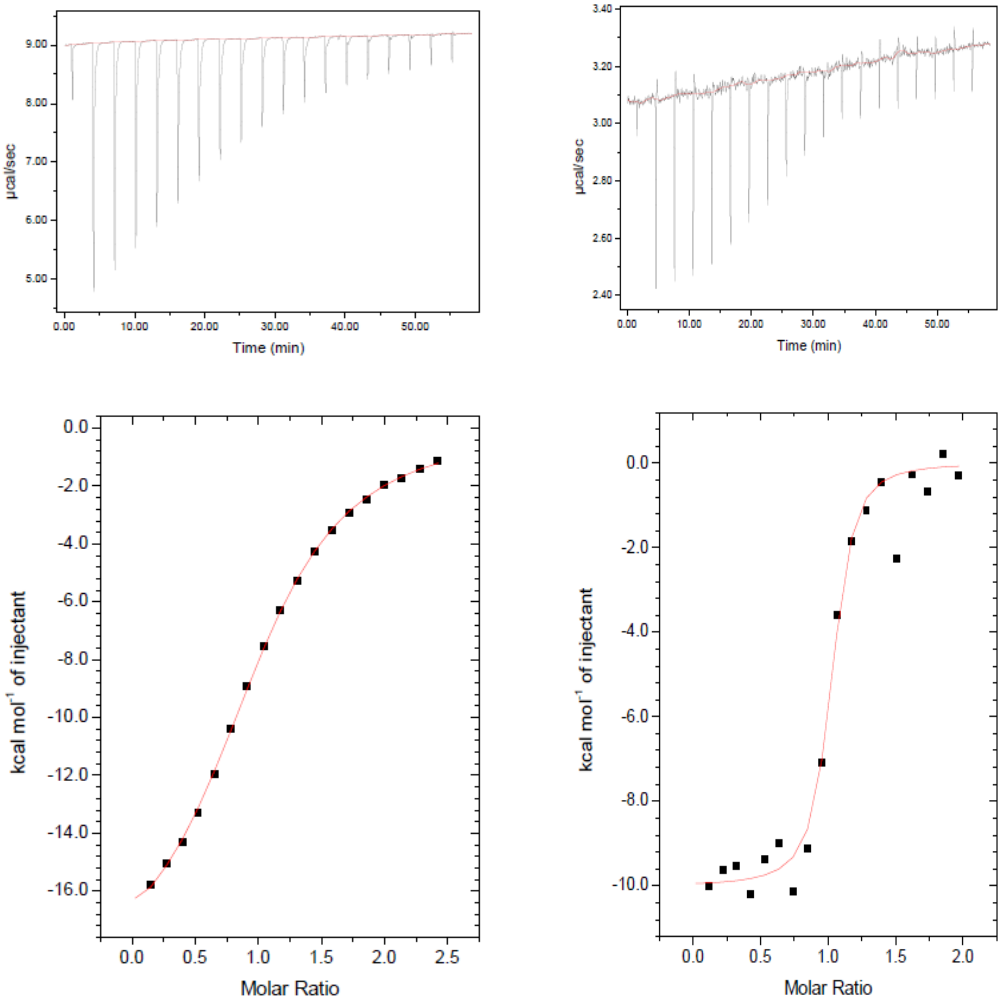

Chart S4. Titration of Oligo-1 into A3A-E72A in high salt (left) and medium salt (right) buffers. The upper panel shows the raw injection data, and the lower panel shows the integrated injection enthalpies after background correction. The solid line in the lower panel represents a fit of the data to a one-site binding model.

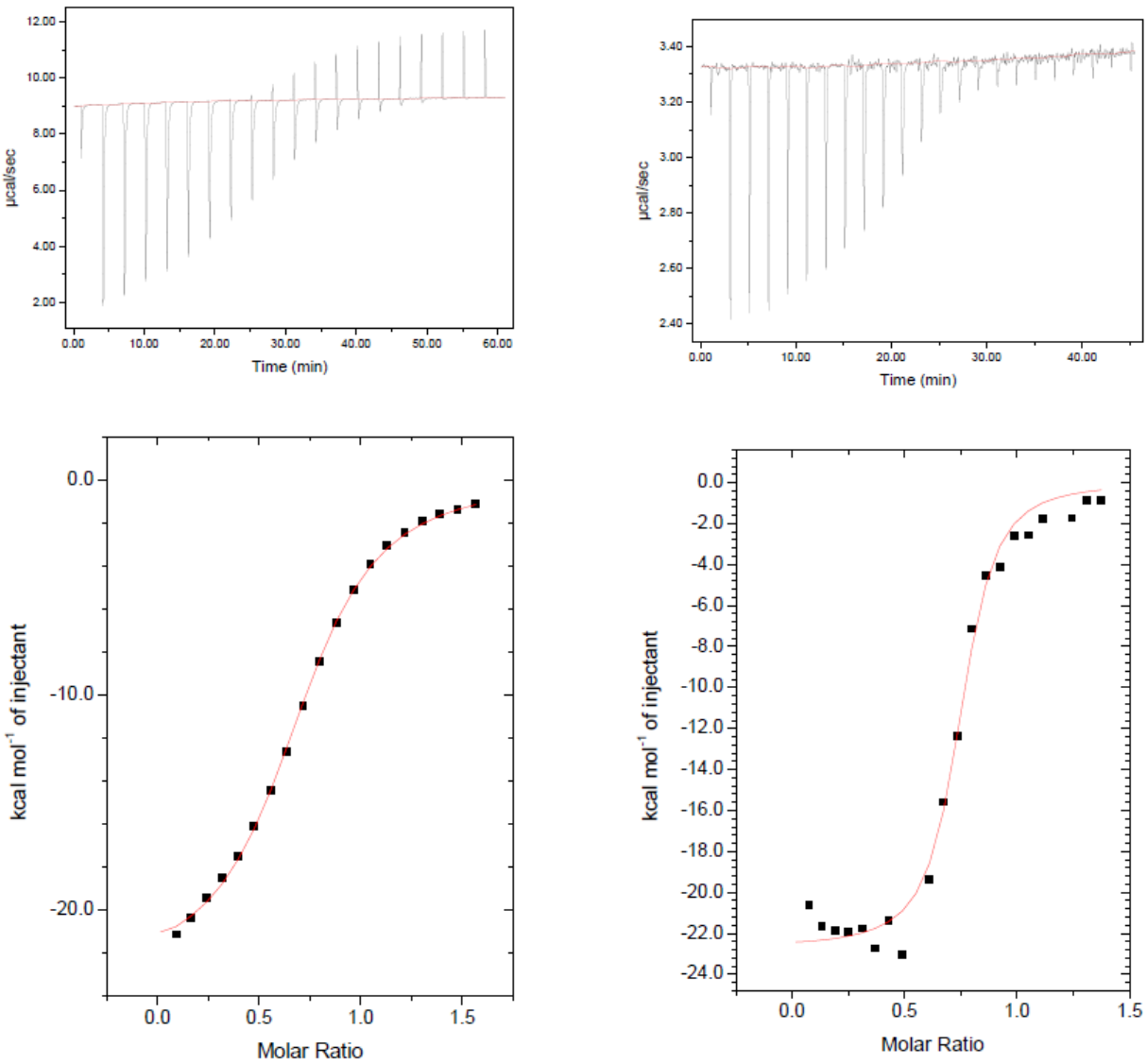

Chart S5. Titration of Oligo-2 into A3A-E72A in high salt (left) and medium salt (right) buffers. The upper panel shows raw injection data, and the lower panel shows integrated injection enthalpies after background correction. The solid line in the lower panel represents a fit of the data to a one-site binding model.

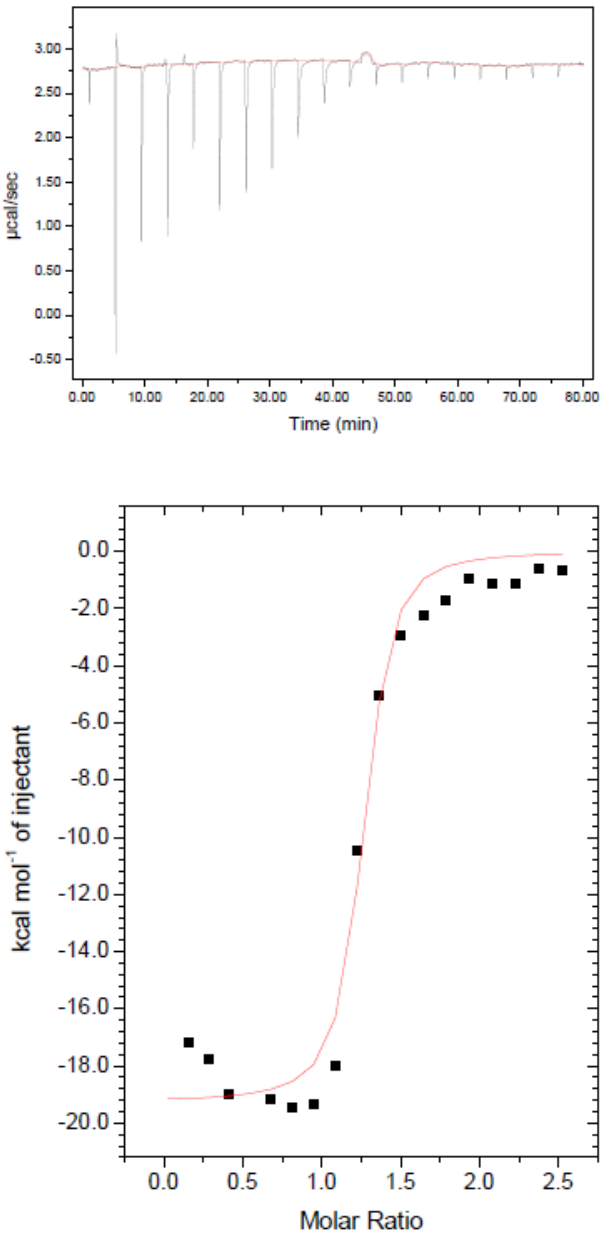

Chart S6. Titration of Oligo-3 into A3A-E72A in a medium salt buffer. The upper panel shows raw injection data, and the lower panel shows integrated injection enthalpies after background correction. The solid line represents a fit of the data to a one-site binding model.

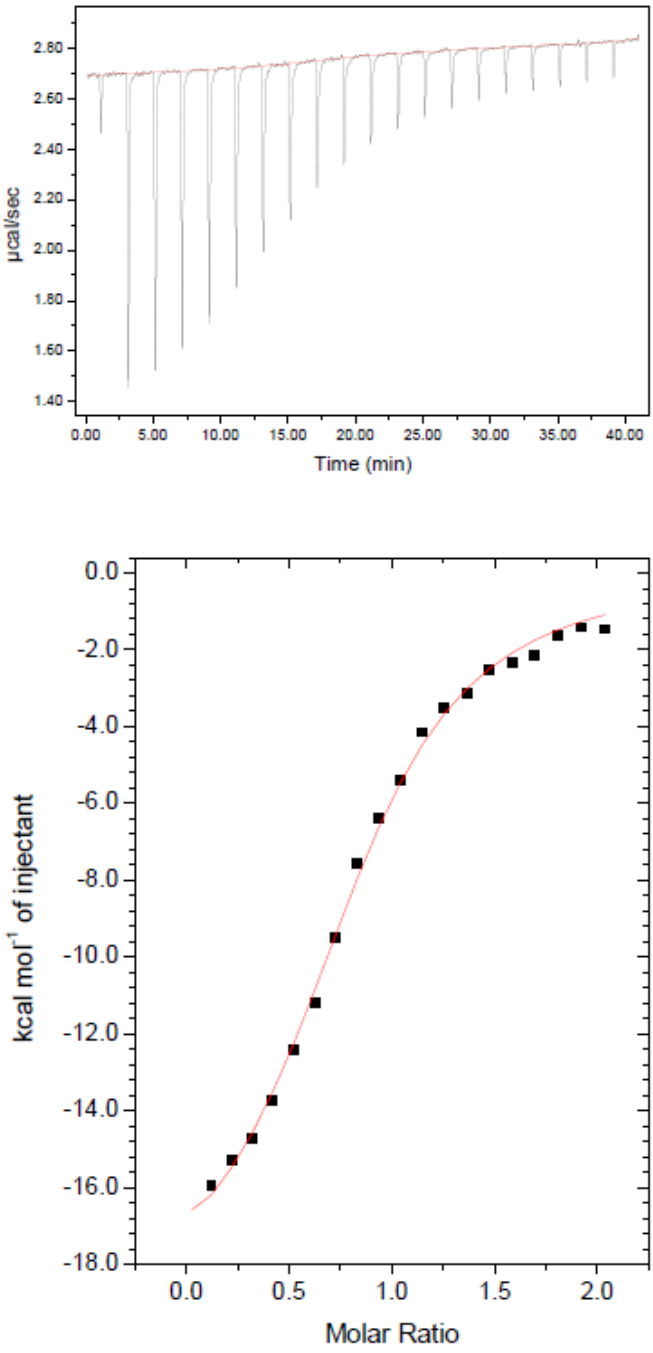

Chart S7. Titration of Oligo-4 into A3A-E72A in a medium salt buffer. The upper panel shows raw injection data, and the lower panel shows integrated injection enthalpies after background correction. The solid line represents a fit of the data to a one-site binding model.

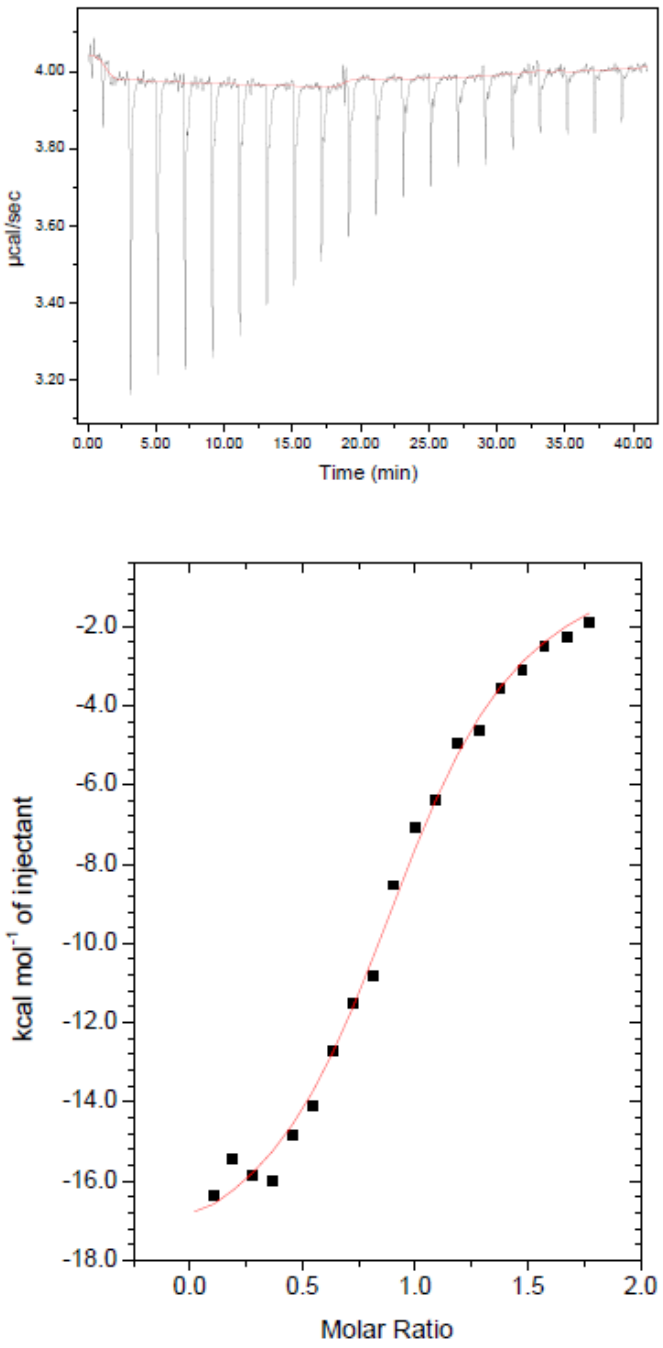

Chart S8. Titration of Oligo-5 into A3A-E72A in a medium salt buffer. The upper panel shows raw injection data, and the lower panel shows integrated injection enthalpies after background correction. The solid line represents a fit of the data to a one-site binding model.

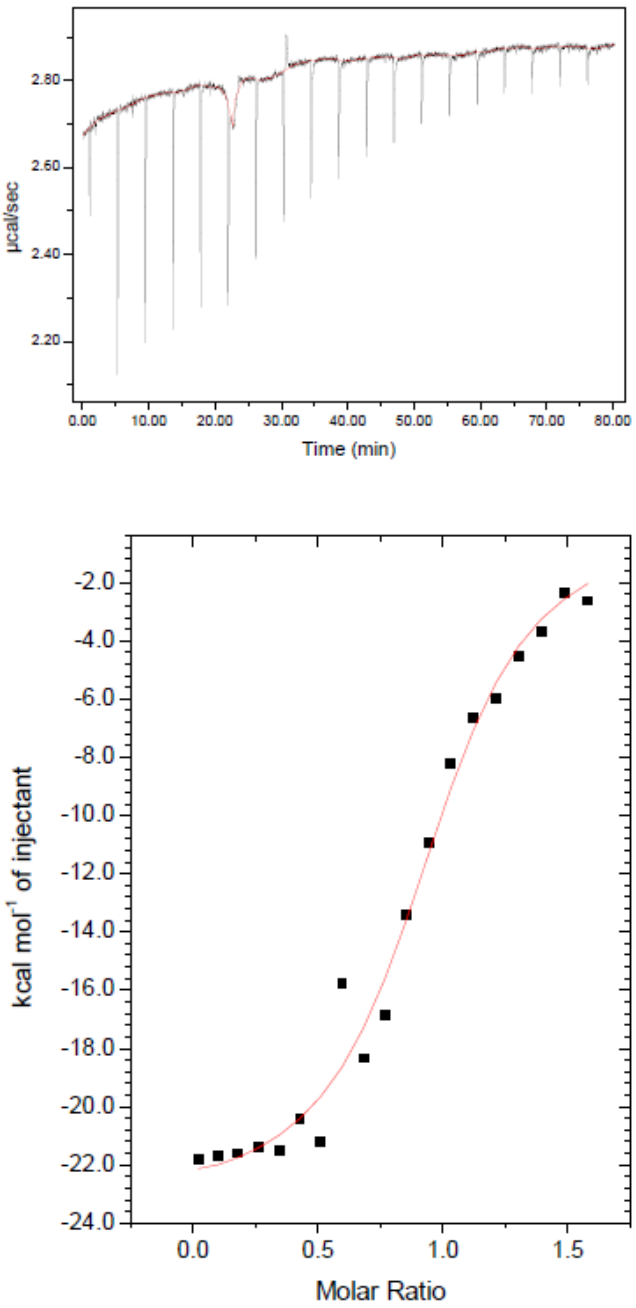

Chart S9. Titration of Oligo-6 into A3A-E72A in a medium salt buffer. The upper panel shows raw injection data, and the lower panel shows integrated injection enthalpies after background correction. The solid line represents a fit of the data to a one-site binding model.

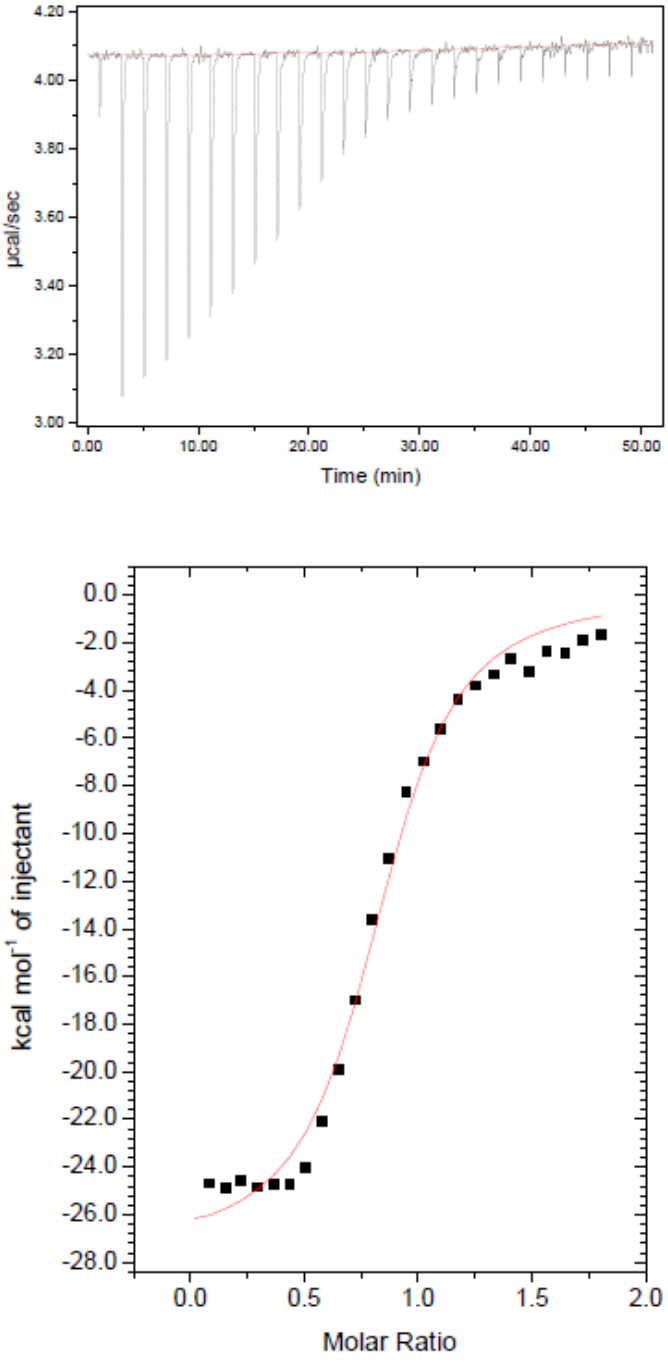

Chart S10. Titration of Oligo-7 into A3A-E72A in a medium salt buffer. The upper panel shows raw injection data, and the lower panel shows integrated injection enthalpies after background correction. The solid line represents a fit of the data to a one-site binding model.

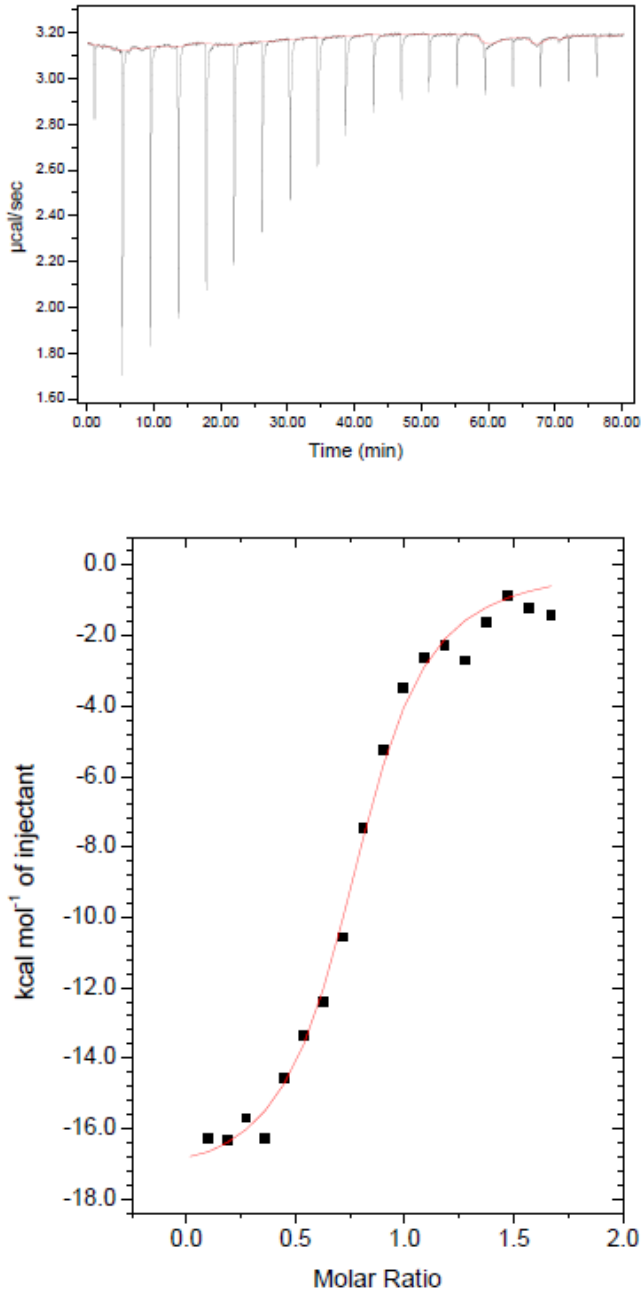

Chart S11. Titration of Oligo-8 into A3A-E72A in a medium salt buffer. The upper panel shows raw injection data, and the lower panel shows integrated injection enthalpies after background correction. The solid line represents a fit of the data to a one-site binding model.

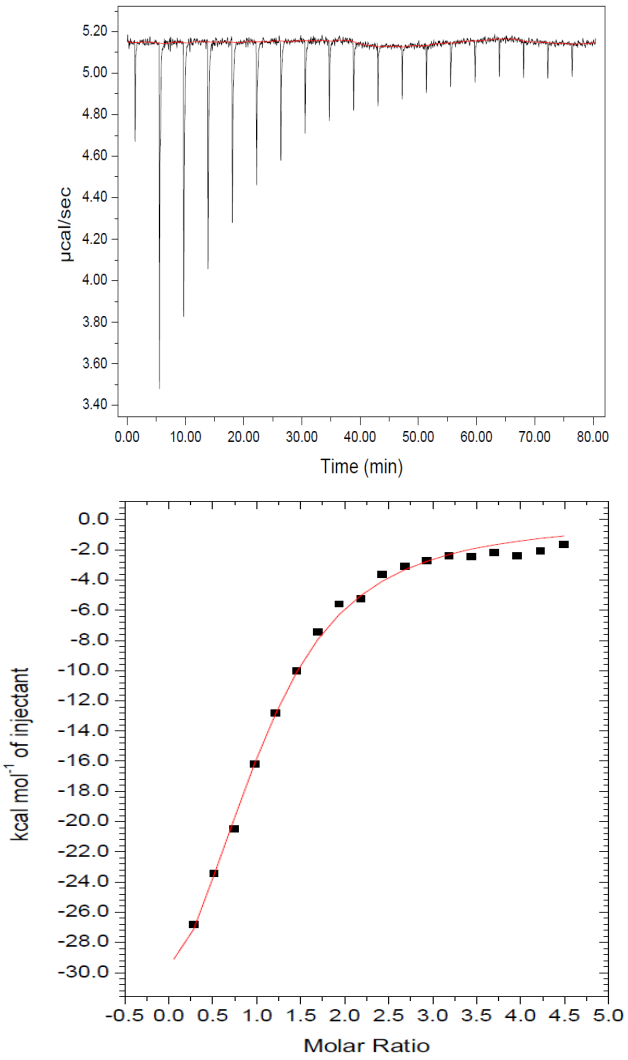

Chart S12. Titration of Oligo-9 into A3B$_{CTD}$-QM-ΔL3-AL1swap in the activity assay buffer. The upper panel shows raw injection data, and the lower panel shows integrated injection enthalpies after background correction. The solid line in the lower panel represents a fit of the data to a one-site binding model.

Table S2. The solid lines in the lower panels of the above charts (**Chart S4 – Chart S12**) of ITC titrations represent fits of the data to a one-site binding model, yielding the following experimental parameters:

Protein/ssDNA	***buffer***	***n***	***K, M^{-1}***	**ΔH, *kcal/mol***	**ΔS, *cal/mol/deg***
A3A-E72A +					
Oligo-1	High salt	1.01	$(4.2\pm0.1)\times10^4$	-19	-44
	Medium salt	0.98	$(9\pm4)\times10^6$	-10	-17
Oligo-2	High salt	0.71	$(3.95\pm0.14)\times10^4$	-23	-56
	Medium salt	0.73	$(5.1\pm1.2)\times10^5$	-23	-45
Oligo-3	Medium salt	1.2	$(4.2\pm1.9)\times10^6$	-19	-34
Oligo-4	Medium salt	0.82	$(2.0\pm0.2)\times10^5$	-20	-41
Oligo-5	Medium salt	1.0	$(3.2\pm0.5)\times10^5$	-21	-44
Oligo-6	Medium salt	0.95	$(2.1\pm0.4)\times10^6$	-23	-49
Oligo-7	Medium salt	0.83	$(1.0\pm0.2)\times10^6$	-27	-64
Oligo-8	Medium salt	0.77	$(5.8\pm0.9)\times10^5$	-18	-33
$A3B_{CTD}$-QM-ΔL3-AL1swap + Oligo-9	Activity assay buffer	1.0	$(1.81\pm0.21)\times10^5$	-42	-116

Table S3. The rationales for the designs of Oligos used in this study:

#	DNA sequence, 5'-3'	Rationale
Oligo-1	AAAAAAAATTCAAAAAAAAA	Positive control as reported[10],
Oligo-2	ATTTCATTT	Used in NMR studies of A3A[17] and $A3B_{CTD}$[18], candidate to insert dZ
Oligo-3	ATTCCCAATT	Used in NMR studies of $A3G_{CTD}$[19] and to compare ITC and FP assays
Oligo-4	TTCCC	To study length effects towards A3 binding, inform the designs of dZ-containing oligos and to compare ITC and FP assays
Oligo-5	CCCAA	
Oligo-6	TTCAT	To study length effects towards A3 binding and inform the designs of dZ-containing oligos
Oligo-10	TTTTCAT	
Oligo-14	TTCAAAAA	
Oligo-7	ATTCC**dZ**AATT	dZ-modified oligos for direct comparison to substrate (Oligo-3) above and to study $A3G_{CTD}$ inhibition
Oligo-8	ATTCC**dZ**^{Me}AATT	
Oligo-9	ATTT**dZ**ATTT	dZ-modified oligo to study $A3B_{CTD}$ inhibition
Oligo-15	TTTT**dZ**AT	Modified oligo for direct comparison to substrate (Oligo 10) above in FP assay
Oligo-16	5'-(6-FAM)TTT TCAT	Fluorescent DNA tracer for FP assays

3.3. Thermal Shift Assay

A fluorescence- based thermal shift assay was used to assess binding capability of ssDNA oligonucleotides to $A3B_{CTD}$ proteins, through examination of changes in the proteins thermal stability. Binding assays were conducted using inactive $A3B_{CTD}$ protein constructs, $A3B_{CTD}$-QM-ΔL3 and $A3B_{CTD}$-QM-ΔL3 (E255A), where dC substrate is not converted to dU, and to determine if differences in binding occur due to a single amino acid change (E255A) in the protein.

Purified $A3B_{CTD}$ protein was appropriately diluted in optimised NMR buffer (50 mM citrate-phosphate pH 5.5, 200 mM NaCl, 2 mM β-mercaptoethanol, pH 5.5, 200 µM 4,4-dimethyl-4-silapentane-1-sulfonic acid (DSS)). Assay experiments were setup in a total volume of 25 µl containing; 20 µM $A3B_{CTD}$ protein, 100 µM ssDNA oligonucleotide, mixed with SYPRO® orange dye (BioRad) at a final concentration of 10X. Assays were dispensed into wells of a white Low-Profile 96-Well plate (Roche) then sealed with optical seal, shaken, and centrifuged. Thermal scanning (20 to 95°C at 0.6°C/min) was performed using a real-time PCR setup on a LightCycler 480 instrument II (Roche) with fluorescence emission spectra recorded with combinations of excitation and emission filters (483–610 and 483–568 nm, respectively).

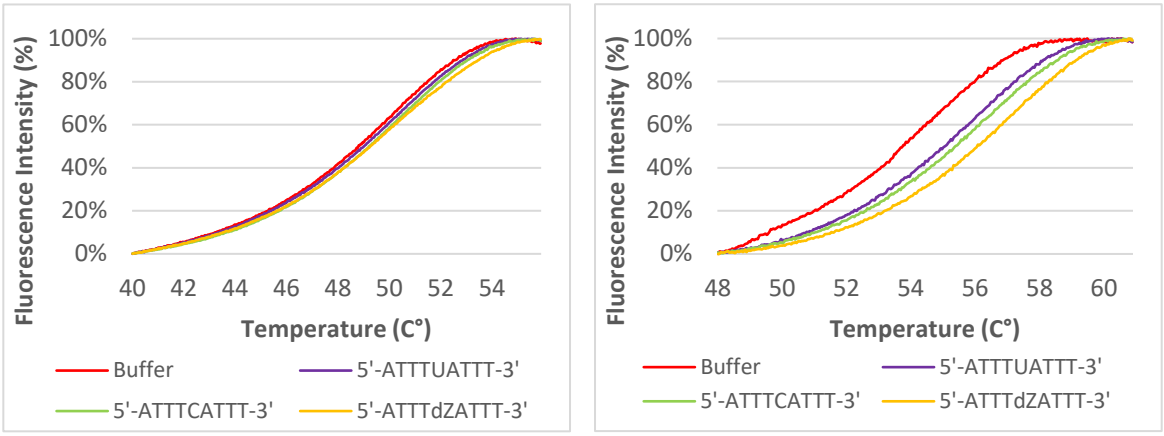

$A3B_{CTD}$-QM-ΔL3- **$A3B_{CTD}$-QM-ΔL3**

Chart S13. Thermal denaturation profiles obtained for $A3B_{CTD}$-QM-ΔL3 (E255A, left) and $A3B_{CTD}$-QM-ΔL3 (right) in the absence (buffer) and in the presence of oligos. The melting temperatures for $A3B_{CTD}$-QM-ΔL3-E255A and $A3B_{CTD}$-QM-ΔL3 in absence of oligo(buffer) are 49.00 ± 0.04 and 54.75 ± 0.33, respectively.

Raw fluorescent intensity data was normalised to percentage, fit to curves, then melting temperature calculation (T_m) was determined at the midpoint (50 %), defined when a protein's melting transition occurs between the folded and unfolded states. Assessment

of binding of the ssDNA oligonucleotides to the $A3B_{CTD}$ proteins were measured by examining the change in melting temperature (ΔT_m) in the presence of oligo compared to absence (buffer) of oligo. Experimental replicates were performed which were analysed using a Q-test for the identification and rejection of outliers based on a 95% confidence interval.

4. Enzymatic assays

4.1. Evaluation of nucleosides by fluorescence-based deamination assay using hA3A and hA3B$_{CTD}$ expressed in HEK293T cells

A3-deaminase activity assays were performed according to Li and colleagues[20] with the following modifications. Stock solutions of nucleosides in molecular biology grade water were serially diluted in protein dilution buffer (10 µL). Recombinant (purified from HEK293T cells) full length A3A-mycHis[20] (10 ng) or C-terminal domain (amino acids 195-382) A3B$_{CTD}$-mycHis[21, 22] (25 ng) proteins were delivered to each well in protein dilution buffer (10 µL). The deamination dual-fluorophoric substrate oligo 5'-(6-FAM)-AAA-TAT-CCC-AAA-GAG-AGA-(TAMRA) (2 pmol) and UDG (25 units) were delivered in TE buffer (10 µL). Cleavage of oligonucleotides containing an abasic site using NaOH (4 M, 3 µL) occurred after 30 min reaction incubation at 37 °C. Plates were read using BioTek Synergy H1 plate reader with an excitation wavelength at 490 nm and emission at 520 nm. Each experiment was performed in biological duplicate with three technical replicates per condition. Resulting total fluorescence values were reported together with the no-protein low control and protein only high control (no inhibitors). nonspecific inhibitor MN-1 was used as a positive control (**Fig. S1**).

4.2. Kinetic characterisation of A3B$_{CTD}$-QM-ΔL3-AL1swap and A3B$_{CTD}$-DM

The kinetic characterization of A3B$_{CTD}$-QM-ΔL3-AL1swap and of A3B$_{CTD}$-DM on dATTT**C**ATTT substrate was conducted using an established one-dimensional proton-NMR (1D ^{1}H-NMR) based assay.[11] This assay utilizes the naturally abundant proton (^{1}H) isotope nuclei within ssDNA molecule and monitors the real-time deamination of the dC (substrate, dATTT**C**ATTT) to dU (product, dATTT**U**ATTT). Measurements were acquired on a 700-MHz Bruker NMR spectrometer equipped with a 1.7-mm cryoprobe at 298 K. A series of ^{1}H NMR spectra was recorded of the oligonucleotide substrate 5'-dATTT**C**ATTT at concentrations ranging from 50 µM to 750 µM with 50 nM of A3B$_{CTD}$-QM-ΔL3-AL1swap protein or 2 µM of A3B$_{CTD}$-DM in a buffer (50 mM citrate-phosphate, 200 mM NaCl, 2 mM β-mercaptoethanol, 200 µM 4,4-dimethyl-4-silapentane-1-sulfonic acid (DSS); pH 5.5 for A3B$_{CTD}$-QM-ΔL3-AL1swap, pH 7.5 for A3B$_{CTD}$-DM) containing 10 % deuterium oxide. The H-5 proton doublet signal of the cytosine, which appears between 5.92 to 5.88 ppm, was baselined and integrated (**Chart S14**, example for A3B$_{CTD}$-QM-ΔL3-AL1swap). A doublet of doublets at 2.57 to 2.39 ppm originating from citrate buffer was used as an internal standard to determine the concentration of substrate converted during the reaction. The integrated signal area was converted to substrate concentration and plotted versus time of the reaction. This plot was then

fitted with linear regression to determine the initial speed of the reaction. **Charts S15** and **S17** show the dependence of speed of the reaction on substrate concentration for $A3B_{CTD}$ -QM-ΔL3-AL1swap and $A3B_{CTD}$ -DM, respectively. The double reciprocal plots (**Charts S16** and **S18**) were then fitted with linear regression to determine K_m, and k_{cat} using the following formula (showing numbers obtained for $A3B_{CTD}$ -QM-ΔL3-AL1swap with enzyme concertation [E] = 50 nM):

$$y = V_0 = k_{\text{cat}}[\text{E}]\frac{[\text{S}]}{K_{\text{m}} + [\text{S}]}$$

$$\frac{1}{V_0} = \frac{K_{\text{m}} + [\text{S}]}{k_{\text{cat}}[\text{E}][\text{S}]}$$

$$\frac{1}{V_0} = \frac{K_{\text{m}}}{k_{\text{cat}}[\text{E}]}\frac{1}{[\text{S}]} + \frac{1}{k_{\text{cat}}[\text{E}]}$$

$$y = ax + b$$

$$b = \frac{1}{k_{\text{cat}}[\text{E}]} = 70.9 \text{ sec } \mu\text{M}^{-1}$$

$$k_{cat} = 0.28 \pm 0.04 \text{ s}^{-1}$$

$$a = \frac{K_{\text{m}}}{k_{\text{cat}}[\text{E}]} = 13960 \text{ s}$$

$$K_{\text{m}} = a / b = 197 \pm 64 \ \mu\text{M}$$

Uncertainties of K_m and k_{cat} were calculated from regression fit (**Chart S16**) using LINEST function of Excel.

Activity data for A3B$_{CTD}$ -QM-ΔL3-AL1swap:

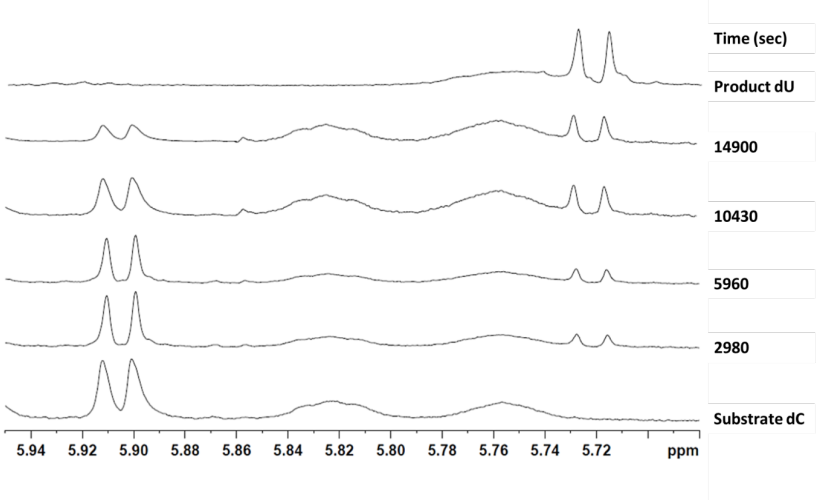

Chart S14. ^{1}H-NMR spectra for the substrate (dAT$_3$CAT$_3$) and its conversion to the product (dAT$_3$UAT$_3$) over time in the presence of A3B$_{CTD}$ -QM-ΔL3-AL1swap (50 nM) at 298 K in activity assay buffer.

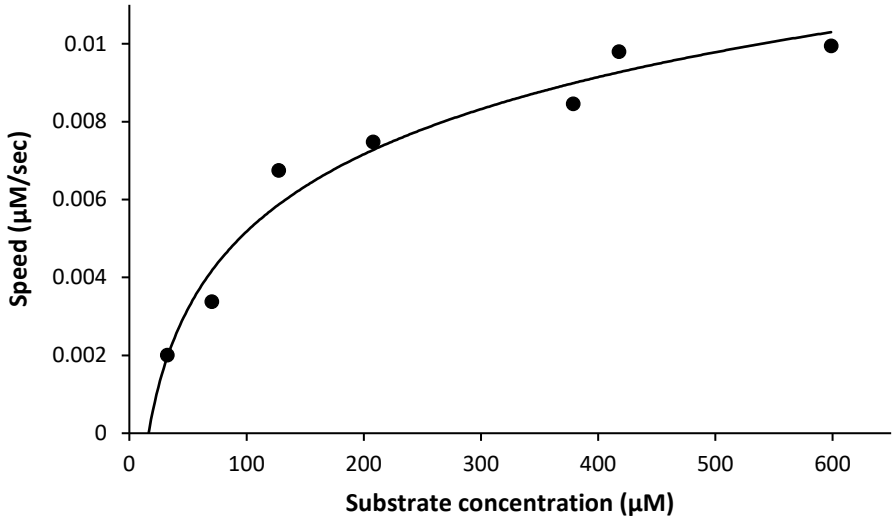

Chart S15. Speed of deamination catalysed by A3B$_{CTD}$ -QM-ΔL3-AL1swap (50 nM) as a function of substrate (dAT$_3$CAT$_3$) concentration.

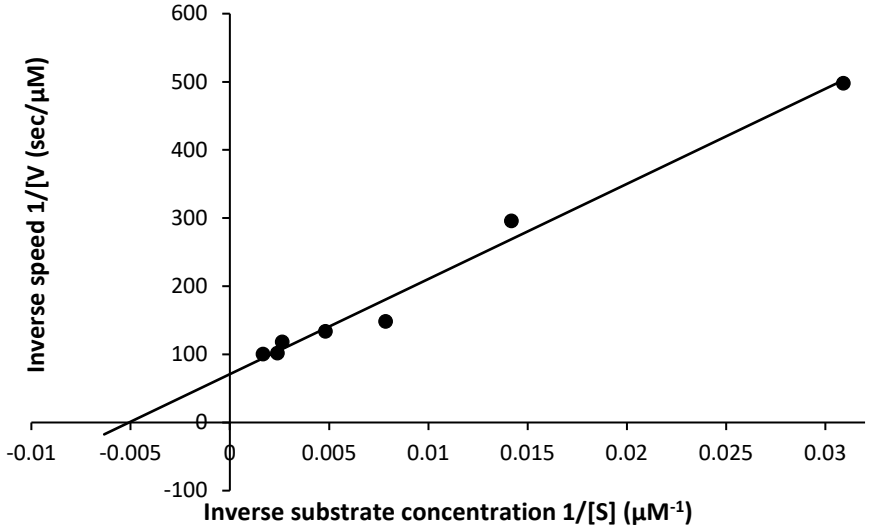

Chart S16. Double reciprocal plot of inversed speed of deamination catalysed by $A3B_{CTD}$-QM-ΔL3-AL1swap (50 nM) as a function of the inversed substrate concentration (dAT_3CAT_3).

Activity data for $A3B_{CTD}$-DM:

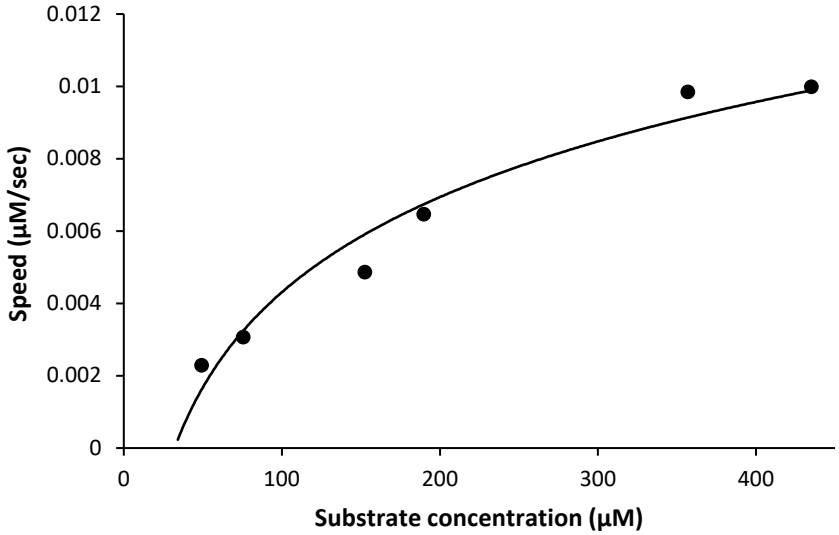

Chart S17. Speed of deamination catalysed by $A3B_{CTD}$-DM as a function of substrate (dAT_3CAT_3) concentration.

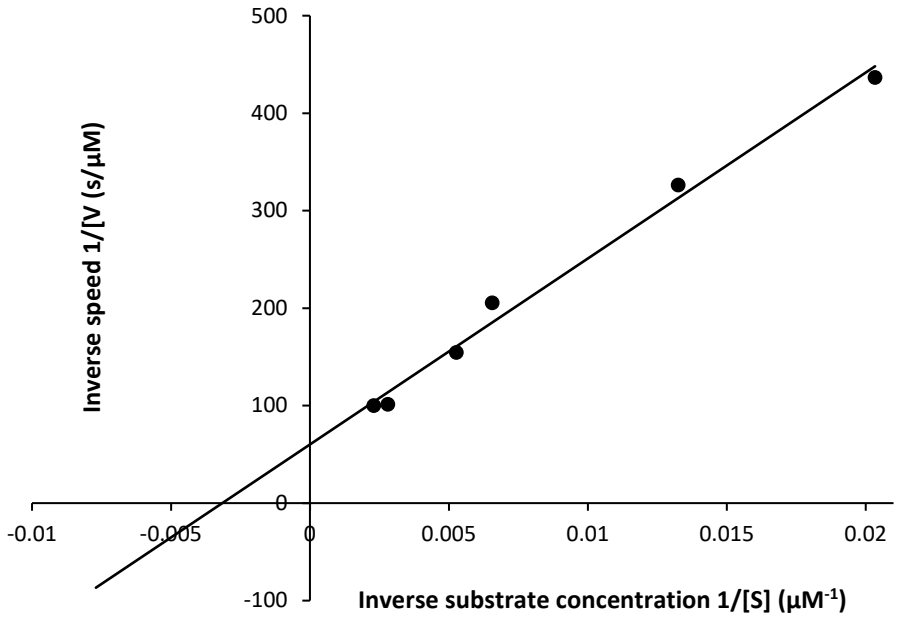

Chart S18. Double reciprocal plot of inversed speed of deamination catalysed by $A3B_{CTD}$-DM as a function of the inversed substrate concentration (dAT_3CAT_3).

4.3.Evaluation of inhibitors in NMR-based assay

4.3.1. Calculation of inhibition of $A3G_{CTD}$ by Oligo-7

Here, we assumed the competitive character of inhibition. For this case, Michaelis-Menten expression for deamination velocity *v* becomes:

$$v = \frac{v_{\max}[S]}{K_{\mathrm{m}}\left(1+\frac{[\mathrm{I}]}{K_{\mathrm{i}}}\right)+[\mathrm{S}]}$$

$$1/v = \left(\frac{K_{\mathrm{m}}}{K_i v_{\max}[\mathrm{S}]}\right)[\mathrm{I}] + \frac{K_{\mathrm{m}}+[\mathrm{S}]}{v_{\max}[\mathrm{S}]}$$

$$y = ax + b$$

$$b = 0.026 \text{ s nM}^{-1}$$

$$a = 2.6\times10^{-4} \text{ s nM}^{-1} \text{ μM}^{-1}$$

$$K_{\mathrm{m}} = 0.57 \text{ mM}$$

$$k_{\mathrm{cat}} = 5.8 \text{ min}^{-1}$$

$$[\mathrm{S}] = 500 \text{ μM}$$

$$[E] = \frac{K_{\mathrm{m}}+[\mathrm{S}]}{bk_{\mathrm{cat}}[\mathrm{S}]} = 850 \text{ nM}$$

$$K_{\mathrm{i}} = \frac{K_{\mathrm{m}}}{ak_{\mathrm{cat}}[\mathrm{E}][\mathrm{S}]} = 53 \text{ μM}$$

where v_{max} is the maximal velocity, K_m and k_{cat} are Michaelis-Menten constants, K_i is an inhibition constant, [S] and [I] are substrate and inhibitor concentrations, respectively.

The $1/v$ dependency on [I] provides a straight line. Two parameters, *a* and *b* (containing K_m, k_{cat} and K_i), can be fitted using the straight line equation ($y = ax + b$).

Using published values of k_{cat} and K_m for the protein,[11] and known [S] = 500 μM, we can calculate [E] and K_i. The value of [E] = 850 nM corresponds to the concentration of enzyme given and serves as additional control. Uncertainty of K_i was calculated using error-propagation method.

4.3.2. Calculation of inhibition of A3B$_{CTD}$-QM-ΔL3-AL1swap and A3B$_{CTD}$-DM by Oligo-9

Based on activity assay described above, measurements of the inhibition of A3B$_{CTD}$-QM-ΔL3-AL1swap and of A3B$_{CTD}$-DM deaminase activity by dZ-containing oligonucleotide were conducted. A series of ^{1}H NMR spectra was recorded of the substrate 5'-ATTTCATTT at constant concentration of 350 µM with varying concentrations of the inhibitor 5'-ATTTdZATTT ranging from 5 µM to 100 µM in the presence of 50 nM of A3B$_{CTD}$-QM-ΔL3-AL1swap or of 2 µM of A3B$_{CTD}$-DM in activity assay buffer as mentioned previously at 298 K. Integration of the H-5 proton doublet signal of the cytosine (between 5.92 to 5.88 ppm) which was then converted to substrate concentration and plotted versus time of the reaction. This plot was then fitted with linear regression to determine the speed of the reaction in the presence of inhibitor. The plot of inverse speed *versus* inhibitor concentration was then fitted with linear regression to derive the inhibition constant (K_i) using the following formula and K_m and k_{cat} values obtained above for A3B$_{CTD}$-QM-ΔL3-AL1swap (numbers shown) and for A3B$_{CTD}$-DM. Uncertainty of K_i was calculated using error-propagation method.

$$v = \frac{v_{\max}[\mathrm{S}]}{K_\mathrm{m}\left(1+\frac{[\mathrm{I}]}{K_\mathrm{i}}\right)+[\mathrm{S}]}$$

$$1/v = \left(\frac{K_\mathrm{m}}{K_i v_{\max}[\mathrm{S}]}\right)[\mathrm{I}] + \frac{K_\mathrm{m}+[\mathrm{S}]}{v_{\max}[\mathrm{S}]}$$

$$y = ax + b$$

$b = 435.0\ \mathrm{s};\ a = 52.96\ \mathrm{s\ \mu M^{-1}};\ K_\mathrm{m} = 197\ \ \mu\mathrm{M};\ [\mathrm{S}] = 350\ \mu\mathrm{M}$

$$K_\mathrm{i} = \frac{K_\mathrm{m} b k_{\mathrm{cat}}[\mathrm{S}]}{a k_{\mathrm{cat}}[\mathrm{S}]\left(K_\mathrm{m}+[\mathrm{S}]\right)} = \frac{bK_\mathrm{m}}{a\left(K_\mathrm{m}+[\mathrm{S}]\right)} = 3.09 \pm 0.93\ \mu\mathrm{M}$$

SI References:

1) Kögler, M., Busson, R., De Jonghe, S., Rozenski, J., Van Belle, K., Louat, T., Munier-Lehmann, H., and Herdewijn, P. (2012) Synthesis and Evaluation of 6-Aza-2'-deoxyuridine Monophosphate Analogs as Inhibitors of Thymidylate Synthases, and as Substrates or Inhibitors of Thymidine Monophosphate Kinase in Mycobacterium tuberculosis, *Chem Biodivers 9*, 536-556.

2) Gottlieb, H. E., Kotlyar, V., and Nudelman, A. (1997) NMR Chemical Shifts of Common Laboratory Solvents as Trace Impurities, *J Org Chem 62*, 7512-7515.

3) Battenberg, O. A., Nodwell, M. B., and Sieber, S. A. (2011) Evaluation of α-Pyrones and Pyrimidones as Photoaffinity Probes for Affinity-Based Protein Profiling, *J Org Chem 76*, 6075-6087.

4) Kotick, M. P., Szantay, C., and Bardos, T. J. (1969) Synthesis of 5-s-substituted 2'-deoxyuridines. Study of the factors influencing the stereoselectivity of the silyl modification of the Hilbert-Johnson reaction, *J Org Chem 34*, 3806-3813.

5) Vives, M., Eritja, R., Tauler, R., Marquez, V. E., and Gargallo, R. (2004) Synthesis, stability, and protonation studies of a self-complementary dodecamer containing the modified nucleoside 2'-deoxyzebularine, *Biopolymers 73*, 27-43.

6) Barchi, J. J., Haces, A., Marquez, V. E., and McCormack, J. J. (1992) Inhibition of Cytidine Deaminase by Derivatives of 1-(β-D-Ribofuranosyl)-Dihydropyrimidin-2-One (Zebularine), *Nucleosides Nucleotides 11*, 1781-1793.

7) Struntz, N. B., and Harki, D. A. (2016) Catch and Release DNA Decoys: Capture and Photochemical Dissociation of NF-κB Transcription Factors, *ACS Chem Biol 11*, 1631-1638.

8) Shi, K., Carpenter, M. A., Kurahashi, K., Harris, R. S., and Aihara, H. (2015) Crystal Structure of the DNA Deaminase APOBEC3B Catalytic Domain, *J Biol Chem 290*, 28120-28130.

9) Shi, K., Carpenter, M. A., Banerjee, S., Shaban, N. M., Kurahashi, K., Salamango, D. J., McCann, J. L., Starrett, G. J., Duffy, J. V., Demir, O., Amaro, R. E., Harki, D. A., Harris, R. S., and Aihara, H. (2017) Structural basis for targeted DNA cytosine deamination and mutagenesis by APOBEC3A and APOBEC3B, *Nat Struct Mol Biol 24*, 131-139.

10) Harjes, S., Jameson, G. B., Filichev, V. V., Edwards, P. J. B., and Harjes, E. (2017) NMR-based method of small changes reveals how DNA mutator APOBEC3A interacts with its single-stranded DNA substrate, *Nucleic Acids Res 45*, 5602-5613.

11) Harjes, S., Solomon, W. C., Li, M., Chen, K.-M., Harjes, E., Harris, R. S., and Matsuo, H. (2013) Impact of H216 on the DNA binding and catalytic activities of the HIV restriction factor APOBEC3G, *J Virol 87*, 7008-7014.

12) Huang, X. (2003) Fluorescence polarization competition assay: the range of resolvable inhibitor potency is limited by the affinity of the fluorescent ligand, *J Biomol Screen 8*, 34-38.

13) Kenakin, T. P. (1993) *Pharmacologic Analysis of Drug-Receptor Interaction*, 2nd ed., Raven, New York.

14) Auld, D. S., Farmen, M. W., Kahl, S. D., Kriauciunas, A., McKnight, K. L., Montrose, C., and Weidner, J. R. (2012) Receptor Binding Assays for HTS and Drug Discovery, In *Assay Guidance Manual [Internet]*, Eli Lilly & Company and the National Center for Advancing Translational Sciences, Bethesda (MD).

15) Rossi, A. M., and Taylor, C. W. (2011) Analysis of protein-ligand interactions by fluorescence polarization, *Nat Protoc 6*, 365-387.
16) Iversen, P., Beck, B., Chen, Y., and al, e. (2004) HTS Assay Validation, (Sittampalam, G., NP, C., and Brimacombe K, e. a., Eds.) Assay Guidance Manual [Internet]. ed., Eli Lilly & Company and the National Center for Advancing Translational Sciences;, Bersheda (MD).
17) Byeon, I. J., Ahn, J., Mitra, M., Byeon, C. H., Hercik, K., Hritz, J., Charlton, L. M., Levin, J. G., and Gronenborn, A. M. (2013) NMR structure of human restriction factor APOBEC3A reveals substrate binding and enzyme specificity, *Nat Commun 4*, 1890.
18) Byeon, I. J., Byeon, C. H., Wu, T., Mitra, M., Singer, D., Levin, J. G., and Gronenborn, A. M. (2016) Nuclear Magnetic Resonance Structure of the APOBEC3B Catalytic Domain: Structural Basis for Substrate Binding and DNA Deaminase Activity, *Biochemistry 55*, 2944-2959.
19) Harjes, S., Solomon, W. C., Li, M., Chen, K. M., Harjes, E., Harris, R. S., and Matsuo, H. (2013) Impact of H216 on the DNA binding and catalytic activities of the HIV restriction factor APOBEC3G, *J Virol 87*, 7008-7014.
20) Li, M., Shandilya, S., Carpenter, M., Rathore, A., Brown, W., Perkins, A., Harki, D., Solberg, J., Hook, D., Pandey, K., Parniak, M., Johnson, J., Krogan, N., Somasundaran, M., Ali, A., Schiffer, C., and Harris, R. (2012) First-in-class small molecule inhibitors of the single-strand DNA cytosine deaminase APOBEC3G, *ACS Chem Biol 7*, 506 - 517.
21) Burns, M. B., Lackey, L., Carpenter, M. A., Rathore, A., Land, A. M., Leonard, B., Refsland, E. W., Kotandeniya, D., Tretyakova, N., Nikas, J. B., Yee, D., Temiz, N. A., Donohue, D. E., McDougle, R. M., Brown, W. L., Law, E. K., and Harris, R. S. (2013) APOBEC3B is an enzymatic source of mutation in breast cancer, *Nature 494*, 366-370.
22) Leonard, B., McCann, J. L., Starrett, G. J., Kosyakovsky, L., Luengas, E. M., Molan, A. M., Burns, M. B., McDougle, R. M., Parker, P. J., Brown, W. L., and Harris, R. S. (2015) The PKC/NF-kappaB signaling pathway induces APOBEC3B expression in multiple human cancers, *Cancer Res 75*, 4538-4547.

SI Figures:

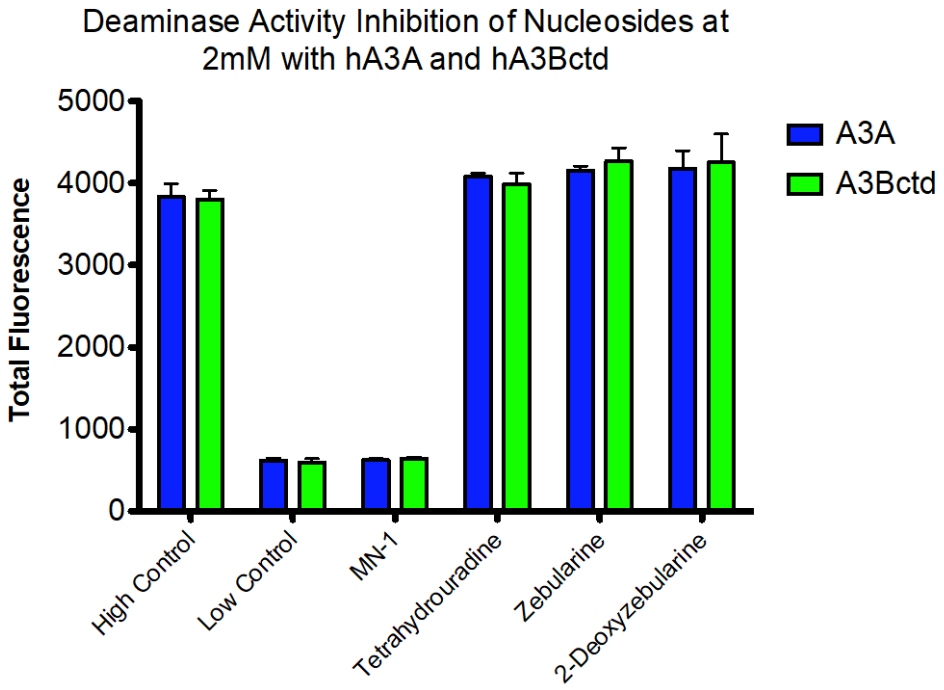

Figure S1. Fluorescence deaminase assays with TSAs (tested at 2 mM; values shown are mean +/- SEM). Low control (no A3 protein), high control (A3 protein without inhibitor). MN-1 is a non-specific inhibitor of DNA enzymes.

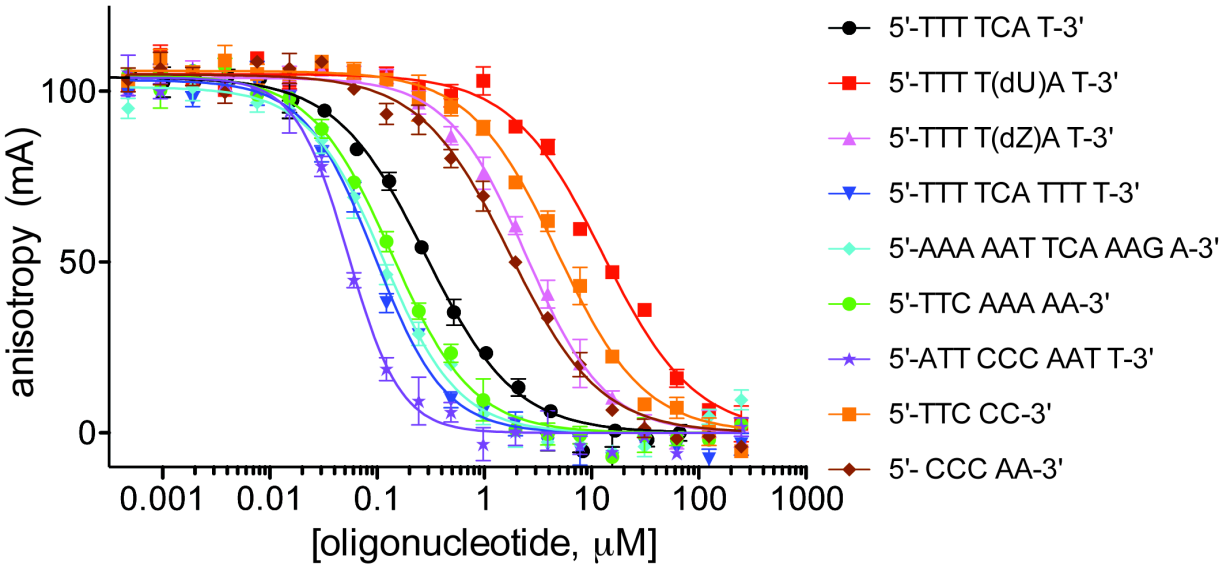

Figure S2. Representative data of fluorescence polarization competition binding assays with oligonucleotides and A3A-E72A.

```
A3G_CTD             ------EILRHSMDPPTFTFNFNNEPWVRGRHETYLCYEVERMHNDTWVLLNQRRGFLCN
hA3A                MEASPASGPRHLMDPHIFTSNFNNG---IGRHKTYLCYEVERLDNGTSVKMDQHRGFLHN
A3A-E72A            MEASPASGPRHLMDPHIFTSNFNNG---IGRHKTYLCYEVERLDNGTSVKMDQHRGFLHN
hA3B_CTD            --------------PDTFTFNFNNDPLVLRRRQTYLCYEVERLDNGTWVLMDQHMGFLCN
A3B_CTDDM           ------EILRYLMDPDTFTFNFNNDPLVLRRRQTYLCYEVERLDNGTWVKMDQHMGFLCN
A3B_CTDQMΔL3        ------EILRYLMDPDTFTSNFNNDPLVLRRRQTYLCYEVERLDNGTSVKMDQHMGFLCN
A3B_CTDQMΔL3AL1     ------EILRYLMDPDTFTSNFNNG---IGRHKTYLCYEVERLDNGTSVKMDQHMGFLCN
A3B_CTDQMΔL3E255A   ------EILRYLMDPDTFTSNFNNDPLVLRRRQTYLCYEVERLDNGTSVKMDQHMGFLCN
                           *  ** ****         *********  * * *   *  *** *

A3G_CTD             QAPHKHGFLEGRHAELCFLDVIPFWKLDLDQDYRVTCFTSWSPCFS--CAQEMAKFISKN
hA3A                QAKNLLCGFYGRHAELRFLDLVPSLQLDPAQIYRVTWFISWSPCFSWGCAGEVRAFLQEN
A3A-E72A            QAKNLLCGFYGRHAALRFLDLVPSLQLDPAQIYRVTWFISWSPCFSWGCAGEVRAFLQEN
hA3B_CTD            EAKNLLCGFYGRHAELRFLDLVPSLQLDPAQIYRVTWFISWSPCFSWGCAGEVRAFLQEN
A3B_CTDDM           EAKNLLCGFYGRHAELRFLDLVPSLQLDPAQIYRVTWFISWSPCFSWGCAGEVRAFLQEN
A3B_CTDQMΔL3        E--------SGRHAELRFLDLVPSLQLDPAQIYRVTWFISWSPCFSWGCAGEVRAFLQEN
A3B_CTDQMΔL3AL1     E--------SGRHAELRFLDLVPSLQLDPAQIYRVTWFISWSPCFSWGCAGEVRAFLQEN
A3B_CTDQMΔL3E255A   E--------SGRHAALRFLDLVPSLQLDPAQIYRVTWFISWSPCFSWGCAGEVRAFLQEN
                           **** * ***..*   **  * **** * *******  ** *   *.  *

A3G_CTD             KHVSLCIFTARIYDD-QGRCQEGLRTLAEAGAKISIMTYSEFKHCWDTFVDHQGCPFQPW
hA3A                THVRLRIFAARIYDY-DPLYKEALQMLRDAGAQVSIMTYDEFKHCWDTFVDHQGCPFQPW
A3A-E72A            THVRLRIFAARIYDY-DPLYKEALQMLRDAGAQVSIMTYDEFKHCWDTFVDHQGCPFQPW
hA3B_CTD            THVRLRIFAARIYDY-DPLYKEALQMLRDAGAQVSIMTYDEFEYCWDTFVYRQGCPFQPW
A3B_CTDDM           THVRLRIKAARIYDY-DPLYKEALQMLRDAGAQVSIMTYDEFEYCWDTFVYRQGCPFQPW
A3B_CTDQMΔL3        THVRLRIKAARIYDY-DPLYKEALQMLRDAGAQVSIMTYDEFEYCWDTFVYRQGCPFQPW
A3B_CTDQMΔL3AL1     THVRLRIKAARIYDY-DPLYKEALQMLRDAGAQVSIMTYDEFEYCWDTFVYRQGCPFQPW
A3B_CTDQMΔL3E255A   THVRLRIKAARIYDY-DPLYKEALQMLRDAGAQVSIMTYDEFEYCWDTFVYRQGCPFQPW
                    ** * *  *****       *.*  *  *** .***** ** .******  ********

A3G_CTD             DGLDEHSQDLSGRLRAILQNQEN
hA3A                DGLDEHSQALSGRLRAILQNQGN
A3A-E72A            DGLDEHSQALSGRLRAILQNQGN
hA3B_CTD            DGLEEHSQALSGRLRAILQNQGN
A3B_CTDDM           DGLEEHSQALSGRLRAILQ----
A3B_CTDQMΔL3        DGLEEHSQALSGRLRAILQ----
A3B_CTDQMΔL3AL1     DGLEEHSQALSGRLRAILQ----
A3B_CTDQMΔL3E255A   DGLEEHSQALSGRLRAILQ----
                   ******** **********
```

Figure S3. $A3B_{CTD}$ and $A3G_{CTD}$ are C-terminal domains of A3B and A3G. $A3B_{CTD}$-DM (double mutant): L230K and F308K, $A3B_{CTD}$-QM (Quadra Mutant): F200S, W228S, L230K, and F308K; $A3B_{CTD}$-QM-ΔL3(loop3 deleted, in text $A3B_{CTD}$-QM-ΔL3): Ala-242 to Tyr-250 →Ser A3B-QM-ΔL3-AL1 (loop 1 swapped with A3A, in text $A3B_{CTD}$-QM-ΔL3-AL1); $A3B_{CTD}$-QM-ΔL3-E255A (in text $A3B_{CTD}$-QM-ΔL3-E255A)-active site glutamate mutated to alanine, A3A-E72A-active site glutamate mutated to alanine.

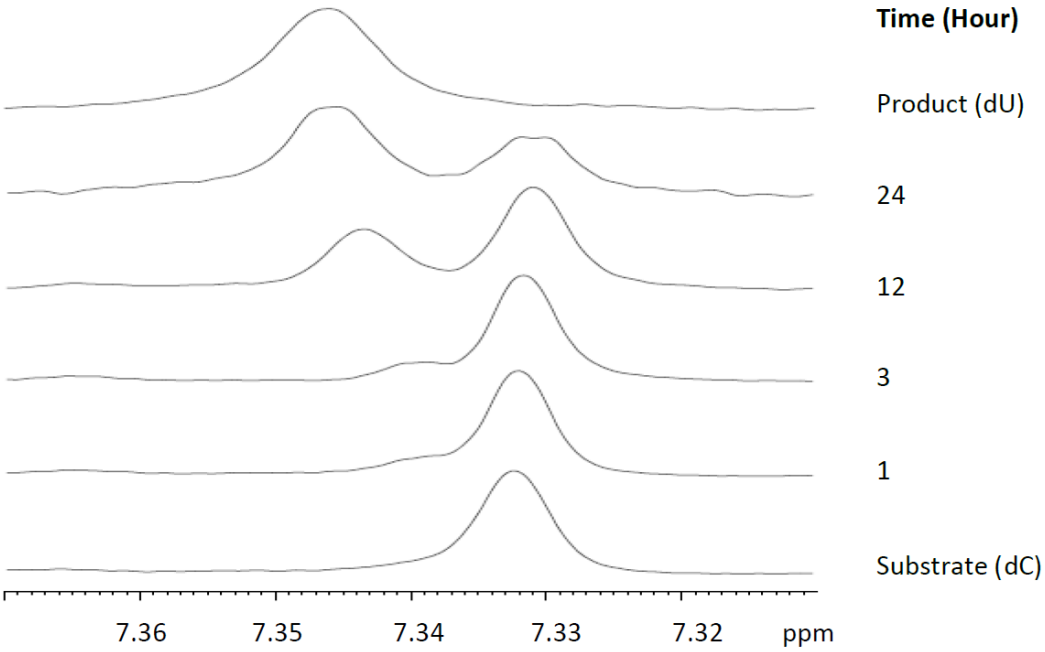

Figure S4. Deamination of dC in 1mM 5'-dAATTCAAAA by the 100 µM of A3Bctd-QMΔL3 protein over time.